# PERFORMANCE BASED DESIGN OF TALL BUILDINGS

**A PROJECT REPORT**

**SUBMITTED IN PARTIAL FULFILLMENT OF THE REQUIREMENTS FOR THE AWARD OF THE DEGREE**

**OF**

**MASTER OF TECHNOLOGY IN**

**STRUCTURAL ENGINEERING**

**SUBMITTED BY**

**NAVEEN JANGRA 2K17/STE/010**

**Under the supervision of Dr. Ritu Raj ASSISTANT PROFESSOR**

**CIVIL ENGINEERING DEPARTMENT**

**DELHI TECHNOLOGICAL UNIVERSITY**

**(Formerly Delhi College of Engineering) Bawana Road Delhi-110042**

**JUNE, 2019**

**DELHI TECHNOLOGICAL UNIVERSITY**

**(Formerly Delhi College of Engineering) Bawana Road Delhi-110042**

# CANDIDATE'S DECLARATION

I hereby declare that the project report entitled "**PERFORMANCE BASED DESIGN OF TALL BUILDINGS"** submitted by me to Delhi Technological University (formerly Delhi College of Engineering) for partial fulfillment of the requirement for the award of the degree of M.TECH in **STRUCTURAL ENGINEERING** is a record of bona-fide project work carried out by me under the guidance of **Dr. Ritu Raj**. I further declare that the work reported in this project has not been submitted either in part or in full, for the award of any other degree or certificate in any other institute or university.

Place: Delhi NAVEEN JANGRA
Date: 30 June, 2019 2K17/STE/012

**CIVIL ENGINEERING DEPARTMENT**
DELHI TECHNOLOGICAL UNIVERSITY
(Formerly Delhi College of Engineering) Bawana Road Delhi
110042

# CERTIFICATE

I hereby certify that the Project Dissertation titled "**PERFORMANCE BASED DESIGN OF TALL BUILDINGS"** which is submitted by **NAVEEN JANGRA (2K17/STE/010)** Civil Engineering Department**,** Delhi Technological University, Delhi in partial fulfilment of the requirement for the award of the degree of Master of Technology, is a record of the project work carried out by the student under my supervision. To the best of my knowledge this work has not been submitted in part or full for any Degree or Diploma to this University or elsewhere.

Place: Delhi
Date: 30 June, 2018

**Dr. Ritu Raj**
Supervisor
Assistant Professor
Department of Civil Engineering
Delhi Technological University

# ACKNOWLEDGEMENT

I want to express gratitude to my mentor, **Dr. Ritu Raj** who gave me the golden opportunity to carry out this beautiful project on the topic **“PERFORMANCE-BASED DESIGN OF TALL BUILDINGS”** which helped me in boosting my technical knowledge and experimental skills. His directions and support were the elemental essences of motivation for me. I feel of the paucity of words to express my sincere thanks to the honorable Head of Department of Civil Engineering, **Dr. NIRENDRA DEV**, for allowing me to utilize the department facilities and have been a constant source of motivation during the course of my project. I express my most profound sense of gratitude towards the Professors of Civil Engineering Department who helped me in formulating the problem statement and clarifying my doubts regarding the project. At last, I would like to thank my colleagues, who helped me by actively participating in discussions and giving their valuable feedback. Their presence and support were invaluable. Finally, I would like to thank my parents for their undying support, motivation and providing me the golden opportunity to study in this prestigious institution.

NAVEEN
JANGRA
2K17/STE/010

# ABSTRACT

Most of the structures designed in the 21st century are based on codes, which follows Forced-Based Design philosophy. The basic intent of the codes is public safety. But there is no information for the losses and interruptions faced by the occupants. Codes focus on designing structures for collapse prevention for design based earthquake. But codes don’t mention the continuity of the operations or non-structural elements damages. Performance based design is a new strategy which is far more detailed focusing on the client specific requirements. In this study a high rise structure is designed following Indian Standards. StructuralTo verify the performance of the structure differnetn types of Pushover Analysis are conducted and the results are compared with the Non-Linear Time Histories (matched with the Indian Response Spectra). Damage states for each member was determined, and nonlinear pushover and time history analysis were carried out using SAP2000 v17.10 to check if story drift ratios meet the ones chosen.

# INDEX

**List of Figures**

**List of Tables**

# CHAPTER 1

## 1.1 INTRODUCTION TO PERFORMANCE BASED BUILDING DESIGN

In the modern era, in urban areas, most of the building are designed following the codes provided by national or state authority. These codes are prescriptive in nature. It is assumed that the buildings designed following the code provisions will perform satisfactorily under the considered earthquake level. The building is designed for the earthquake forces neglecting the site-specific properties. The behavior of the designed building isn't cross verified. Earlier it was tough to verify and match the true nature of the structure if it matches the desired behavior. Put now fast computers and high-end computer programs have made it possible. In Performance-based design methodology, building is designed against a desired (as per probabilistic methodology) level of hazard. This method of the design process is very client specific and dynamic in nature.

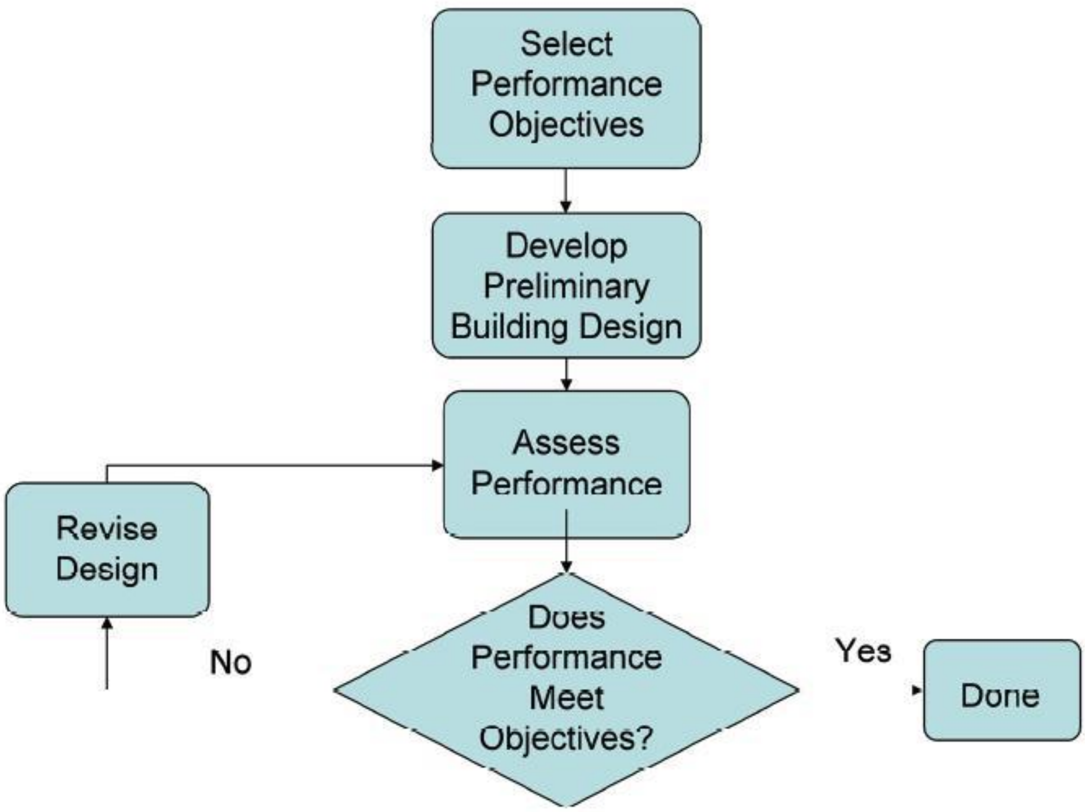


**Fig 1**

*(ATC 1997a)*

## 1.2 Feature of Performance-Based Design

The performance-based design methodology is different from the prescriptive method of design. While prescriptive based design doesn't involve the client in the process and doesn't even consider the requirements of the client, the performance-based design is totally client requirement specific. In this process, before design begins, the client has to define its requirements. These requirements are recorded in the construction document. Requirements can be for protection against Fire, Earthquake or any other kind of hazard.

## 1.3 Why Performance-Based Design

Earthquakes can cause not only structural but non-structural damage also to buildings. Code provisions only provides safety for structural damage. Most of the codes used worldwide, includes only two performance criteria. One is no damage at service level earthquake and another one is no collapse against Design level earthquake. But in Performance Based Design three to four damage states are defines.

A client mat specifies no damage at service level earthquake and damage not exceeding a certain percentage cost of building for repair work. For a Nuclear Power Reactor, it can stated as no damage at service level earthquake and safely closure or reactor at design or maximum considered earthquake. For a tall building, it can involve another criterion of response acceleration at floor level not exceeding a specific limit. Client may also specify to follow damage criteria which follows an insurance industry.

In modern era, more and more high rise building are constructed because of the scarcity of the land. The tall buildings are not only a requirement but also a status symbol of a society. These tall structures are not necessarily to be symmetric following codes. These skyscrapers are masterpieces of architect's imagination having many challenges for a structural engineer. Codal provisions can't be fully satisfied while designing these structures as they involve soft stories, asymmetry in plan and elevation. To make such structures stable under the influence of lateral loads engineers includes dampers, outriggers and other features which can't be designed following codes.

For Indian Standards, the design process becomes more difficult, as in Indian Standards like 1893 earthquake is not defined following probabilistic hazard approach. In IS 1893 earthquake hazard is defined following MSK (modified mericillie scale), which isn't the best way. Design base shear calculated as per IS1893 can be conservative for some situations and for other desired Performance objectives will be far less. Base shear distribution is also based on first mode shape. So the selection ,scaling of earthquake acceleration time histories for analysis becomes more difficult. So, under such circumstances Performance Based Design becomes a need for designing a special structure.

### 1.4 Comparison of Results

Building seismic performance evaluation is the process of comparing and matching the performance of the designed structure against the documented criterion by the client. The structure/building is modified until the requirements demanded by clients are matched. The performance objectives are listed during the preparation of the construction document.

### 1.5 Construction Document

At the initial stage of the project, a document is prepared in which the client's requirements are recorded. In the information of this document regarding the Building's behaviour under different levels of Hazards are mentioned as required by the client. The hazard may have posed by Fire, Wind Loads, Explosion, Earthquake or any other. These requirements are called Performance objectives/Key Performance Indicators/ Performance levels. But the focus of this report is only for Seismic forces.

### 1.6 Statements of Requirements (SoR)

The SoR represents a reference mentioned in the construction. The SoRs is a document, prepared by clients team indicating the client's functional needs. These user-specific requirements are converted into performance requirements. This document includes information about what is essential to the client. The SoRs is dynamic and adds more and more details as projects proceed.

### 1.7 SEISMIC HAZARD LEVELS

Indian standard (***IS 1893 Part 1, 2016***) specify maximum considered earthquake depending on the location of the structure. The code has divided India into five zones ranging from Zone 1 to Zone 5. For each zone peak, ground acceleration is defined. The structure is designed for the design level earthquake which equals to half of the maximum considered earthquake. For zone 5 peak ground acceleration is 0.36 $m/s^2$.

But in the case of PBBD, a different strategy is prepared. The work involves probabilistic seismic hazard analysis and development of response spectra and scaled ground motions for design and analysis. In ***FEMA 356*** three levels of hazards are considered depending on the Probabilistic Earthquake Hazard analysis.

| Probability of Exceedance | Mean Return Period(Years) |
|---|---|
| 50% / 50 Years | 72 |
| 20% / 50 20% / 50 Years | 225 |
| 10% / 50 Years | 474 |
| 2% / 50 Years | 2475 |

*Table 1*

## 1.8 TARGET PERFORMANCE LEVELS (FEMA 356)

A Performance level implies a state of damage, describing the degree of damage absorbed by the structure under a degree of seismic hazard. A performance objective is defined by selecting a desired performance levels (extent of damage)for a given level of earthquake ground motion.

The four-building performance levels are given below:

- Operational
- Immediate Occupancy (IO)
- Life Safety (LS)
- Structural Stability/ Collapse Prevention (CP)

#### 1.8.a Operational (1-A)

- Degree of damage related to continuation of functionality.
- Structural damage is limited so that continued safe occupancy is also minor to non-existent
- Similarly, damage to non-structural elements is also negligible.

| | | TARGET BUILDING PERFORMANCE LEVELS | | | |
|---|---|---|---|---|---|
| | | Operational Performance Level(1-A) | Immediate Occupancy Performance | Life Safety Performance Level(3-C) | Collapse Prevention Performance Level(5-E) |
| Earthquake Hazard Level | 50%/ 50 Years | a | b | c | d |
| | 20%/50 Years | e | f | g | h |
| | BSE-1 (~10%/50 Years) | i | j | k | l |
| | BSE-2 (~2%/50 Years) | m | n | o | p |

*Table 2*

*(FEMA 356)*

#### 1.8b Immediate Occupancy (1-B)

Performance Level 1-B, immediate occupancy, stated as the post-earthquake damage state, indicating structure to remain safe to, especially no degradation in the stiffness of lateral load resisting elements.It is the most widely used performance criteria for a service level earthquake hazard.

#### 1.8c Life Safety (3-C)

- Significant damage to structural elements
- Low probability of progressive collapse
- Very low threat to occupants life

#### 1.8d Structural Stability/ Collapse Prevention (5-E)

- Significant damage to structural elements
- Considerable residual drift

#### 1.8e Basic Safety Objective

Structures satisfying BSO are expected to sustain low damage from service level earthquakes, moderate earthquakes, but are significantly damaged under exceptional level earthquake hazard.

### 1.9 Enhanced Performance Objective

The level which provides building performance more than that of BSO. Normally this level of Performance includes more than one level of performance for different degree of hazard. Sometimes it also includes the repair cost in the fraction of cost of buildings.

### 1.10 Earthquake Ground Motion

- Serviceability Earthquake(SE): 50 % Probability of exceedance in 50 years
- Design Earthquake(DE): 20 % Probability of exceedance in 50 years
- Maximum Considered Earthquake (ME):  2% chance in 50 years

For structures of Ordinary Importance

Life Safety = Design earthquake = (2/3)*MCE

Collapse Prevention = 1.5* MCE

# CHAPTER 2

# LITERATURE REVIEW

**Cruz, C., & Miranda, E. (2017)** In his study Cruz concluded that for a structure vibrating in the higher modes, damping is also higher as compared to the fundamental mode of the vibration. Cruz studied a total of 14 high rise structures against 41 seismographs. The high damping might be because of the soil-structure interaction effect (radiation damping increases with increasing frequency).

**Charilaos. A et al. (2013)** explained the effect of high frequency modes on response of structure. Normally same response reduction factor is assumed for all modes of vibration, even though it is a proven fact that higher modes of vibration are affected unequally. Code based design methods are based on the assumption that structure vibrates in fundamental mode, neglecting the effect of high-frequency modes. Because of this story shear forces are highly nder estimated. Results indicate that in higher modes shear demand in the upper story are highly amplified and acceleration in upper stories, in higher modes are underestimated.

**Dhileep. M, Trivedi. A et al. (2011)** Pushover analysis is generally used as an alternative to NLTHA. However, in pushover analysis high frequesncy modes of vibration are ignored, and the lateral force is assumed to be proportional to mas at story level. In order to take account of higher modes, structural engineers should include high-frequency modes in pushover analysis. If high frequency modes are considered, Pushover analysis resuts are approximate to Non Linear Time History results. This process is also called Modal Pushover analysis.

**A. Shuraim et al., (2007)** As per his work code calculated earthquake forces were not enough to describe the behavior the structure. He showed that most of the vertical load bearing elements did require additional reinforcements when designed following codes. He found that the damage pattern for a structure designed following codes and analyzed for pushover was different which could have been due to discrepancies in code predicted behavior because codes don't define the post-elastic element behavior. In ATC 40 post elastic damage criteria are mentioned. Shuraim also suggested that Pushover analysis shouldn't be applied ignoring engineering judgment after comparing the results.

**Modal Combination Pushover Analysis**

For the Modal Pushover combination analysis, the different mode shapes are combined depending on the mass participation ratio of the structure under different modes and the mass at the corresponding story level. The equation proposed by **Erol KALKAN and Shashi K. KUNNATH** is used to combine modes for calculating the lateral forces at different story levels.

$$F_j = \sum \mathrm{T}_n m \phi_n S_a \ldots\ldots\ldots\ldots\ldots\ldots\ldots\ldots\ldots\ldots\ldots\ldots 1$$

Where T $= modal\ mass\ participation\ ratio\ in\ mode\ n$
M= mass at the story i

$$\phi n = mode\ shape\ for\ the\ mode\ n$$

$S_a$ = spectral acceleration at the period corresponding to mode n

**Chopra and Goel (2001)** developed improved static procedure considering the contribution of different modes of vibration, named as **Modal Pushover Analysis (MPA)**. In this method, the lateral force is applied proportional to the mass at the story, mode shape and square of the angular frequency. The accuracy of the MPA Procedure with respect to the FEMA 356 Nonlinear Static Procedure (NSP) was evaluated by comparison with nonlinear response history analyses of this existing structure. Most of the nonlinear static methods are restricted to 2D frames analyses of symmetric building applicable on buildings with the coincident center of mass and rigidity. To evaluate plan asymmetric buildings, a 3D model is required to capture lateral-torsional response. For evaluation of seismic behavior of complex tall asymmetric buildings having higher mode participation effects, a 3D nonlinear response history analysis is the quite rigorous and accurate method. In such cases Modal Pushover Analysis procedure becomes an attractive option because it achieves a satisfactory balance between accuracy and practicality. In the MPA , the seismic response of a structure is determined by pushing building in each mode to its “modal” target displacement. The overall structural response is obtained modal combination of response of structure. The fundamental is that uncoupling and superposition of modal responses in an inelastic building system is accurate enough for an approximation of peak structural response.

**Peter Fajfar(2000)** Peter Fajfar proposed a simplified nonlinear procedure for 2D concrete structural frames. This philosophy is also known as the N2 speially in EU .This N2 method is totally different from normal pushover analysis method. N2 method gives sufficiently accurate results for the structures vibrating in the first mode. Initially N2 method was presented forregular structures. In this method two different models are created. In the first step stiffness, strengths and ductilities of the structures are calculated. In the second step an equivalent SDOF system having same stiffness, strengths are proposed.Characteristics of this equivalent system are dependent on the Base shear vs roof displacements. In thrid step non linear dynamic analysis is conducted. This can be done by performing non linear spectra.

**FEMA 356, 2000.** Published in the year 2000 by Fedral Emergency Management and Authority, is for a prestandard for the seismic rehabilitation of the structures. In chapter 6 it provides the acceptance criterion, modeling of the elements and plastic hinges for concrete. It is one of the most reliable and most widely used in the industry. Perform 3-D, Computer and Structures has included this to model beams and columns as default.

**Fenwick, R & Dely, R & Davidson, B. (1999).** Fenwick’s work proved that in beams dominated by gravity loading , two types of plastic hinges are formed which are named as reversing and non reversing. The moment direction in non rreversing hinge doesn’t change as the direction of the lateral force reverses in the other half cycles. Beause of this, non eversing hinges doesn’t dissipates energy in the form hystresis.

**Naeim and Lobo (1998)** attempted to identify some short comings of a pushover analysis and summarised important points supposed to be considered preceding the analysis. These were:

The importance of the loading shape function. Lateral force distribution for code provsions, Normal pushover and modal pushover are totally different. Lobo and Naeim checked the effect of different load patterns Uniform, Triangular, FEMA. Results showed that all the different load patterns yielded different results.

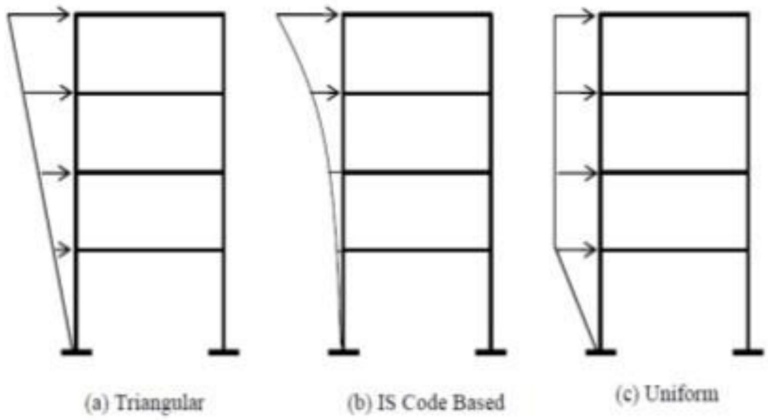


Lateral load pattern for pushover analysis as per FEMA 356
(Source: Jan, T.S.; Liu, M.W. and Kao, Y.C. (2004), "An upper-bond pushover analysis procedure for estimating the seismic demands of high-rise buildings". *Engineering structures.* 117-128)
26

Fig3

**Kilar and Fajfar (1997)** tested the applicability of the proposed method **(Kilar et al., 1996)** on a 21-story structural wall. Reults indicated that for an asymmetric building need to be more ductile if its desired bahvior is similar to the symmetric one.This tools proved to be very effective in predicting the global damage pattern and sequence of the plastic hinge formation in a structure

**ATC40 [13]** This is one of the first code ever published by the applied technological council. This code published the three methods of pushover analysis which are known as method A, method B, method C. Firs two methods are very complicated. Method C is very famous because it is graphical.

In this method, the lateral load is applied up to the point of failure of the structure (Negative stiffness). The Base Shear v/s roof displacement is plotted which is called capacity cure. This capacity curve is converted into ADRs(acceleration displacement response spectra) curve. The demand curve is formed from dynamic response spectra. In this method code based response spectra(without response reduction method) is used to plot the demand curve. The point of intersection is called performance point.

**Ramatani et al.** attempted to characterize the effect tension when the element is loaded under cyclic compressive loads. The test results indicated that once a crack is formed due to tensile stress, to close the crack completely compression is required. Once the crack is closed completely, the stiffness of concrete is not affected by the accumulated damage due to the tension.

# CHAPTER 3

# THEORY of PUSHOVER

Following are the main methods of analysis

- Linear static (termed “lateral force” method).
- Linear modal response spectrum analysis.
- Nonlinear static analysis (“pushover”).
- Nonlinear dynamic (response time-history).

## 3.1 Pushover Analysis

### Why Pushover Analysis?

As elatic analysis can't compute inelastic displacements hence its not an option for predicting the true nature of the structure. Non-Linear time history analysis requires a lot of computing capacity hence that can not be the first option. So, Pushover analysis is the best shot for assessing the real behavior of the structure. In Pushover analysis, a non-linear model is developed and is subjected to gravity loads first followed by monotonically increasing static lateral load. The lateral load pattern is user-defined. Pushover analysis only predicts the most probable pattern of the plastic hinge formation. Pushover analysis may provide a reasonable assessment of the location of the plastic hinges, but the fundamental problem is how far to push the structure?

In pushover analysis, the structure is subjected to an incremental lateral force to achieve a target displacement. Plastic hinges are modelled at the ends of beams and columns as lumped plasticity. As thre structure is displaced in the lateral direction, hinges starts to form near the beam-column joints. This increases the ductility of the structure and hence the effective time period of the structure is also increased. Pushover analysis gives the assement about the damage pattern of the structure. Due to the incremental lateral load, the structure keeps on displacing in the lateral direction upto a certain point, after that structure becomes unstable. All of this depends on the state of the hinge which depends on force deformation curve of the element.

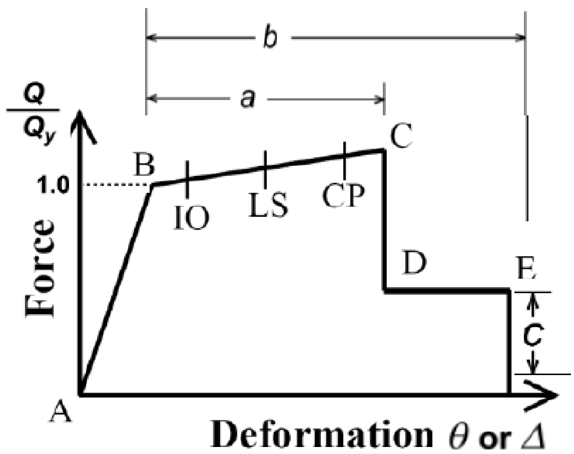


*Fig 3*

As indicated in the above diagram, the force-deformation curve for an element is bilinear, as per FEMA 356.

IO (immediate occupancy)

LS (Life Safety)

CP (Collapse Prevention)

All of these are the performance levels for individual elements.

Following are the methods for Pushover analysis

- Capacity spectrum method, CSM (ATC-40 1996)
- Displacement coefficient method, DCM (FEMA 273 1997)
- Secant method (COLA 1995)
- N2 method (Fajfar 1999, 2000) M
- Modal pushover analysis (Chopra and Goel 2001).

### 3.1.1 Capacity Spectrum Method

Capacity spectrum method is a seismic analysis technique, developed initially by **Freeman et al. (1975)**. Graphical form of this procedure is most commonly used for estimating the structure load-deformation characteristics. This method is also mentioned in the ATC-40 (1996) and FEMA 440 as a displacement-based designmethod. The conceptual development of the CSM is explained in detail in the ATC-40 document. In ATC-40, there are three methods explained as method A, B, and C. The capacity of the structure is compared with the demand imposed by the lateral forces. As the demand (lateral force) increases the structure yields, subsequently stiffness of the structure also decreases and the period lengthens. Capacity curve converted to the ADRS format is named as capacity spectrum , shown in Figure

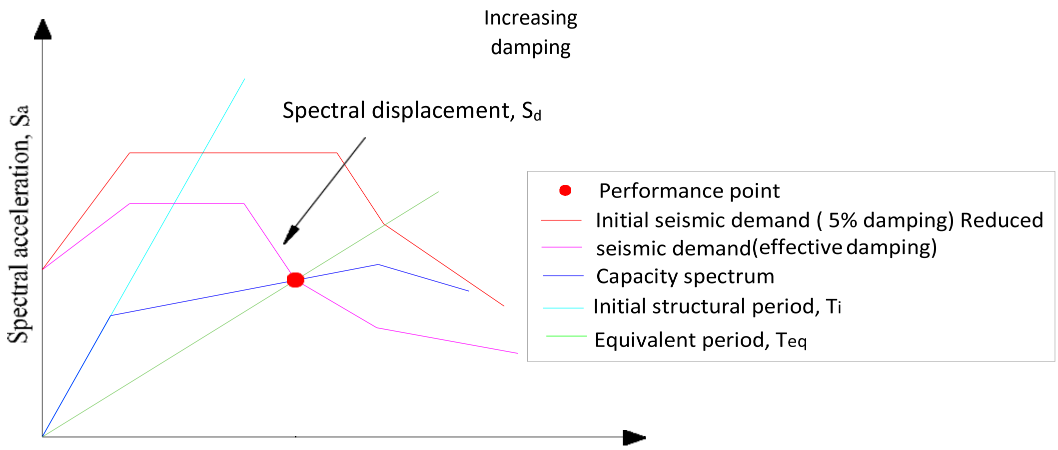


Fig 4

As the structure of building starts to yields, it starts dissipating energy with hysteretic damping. Structures with large hysteresis loops (without pinching) dissipate more energy. Pinched loops are caused by strength and stiffness degration. Because of the energy dissipation,the vibrational enegy isn't needed to be stored in the structure. Which leads to lesser demand compelled on the structure.

### 3.1.2Effective damping (Beff)

When a structure vibrated in inelastic mode, its damping is combination of the inherent viscous damping and the damping caused by the hystersis. Hysteretic damping is proportional to the area of hystrstic loop. Anil K Chopra showed in his work that hystristic damping can represented as equivalent viscous damping. The equivalent viscous damping, $B_{eq}$ , estimated from the following equation

$$B_{eq} = B_o + 0.05 \quad \ldots\ldots\ldots\ldots\ldots\ldots\ldots\ldots\ldots2$$

.

Where $B_o$ = hysteretic damping represented as viscous damping
And as per Anil K. Chopra

$$Bo = \left(\frac{1}{4pi}\right)\frac{E_D}{E_{SO}} \quad \ldots\ldots\ldots\ldots\ldots\ldots\ldots\ldots\ldots\ldots\ldots3$$

Where
$E_D$ = energy dissipated in a single cycle of motion or area of hysteresis loop
And

$E_{so}$ = maximum strain energy associated with cycle of motion i.e area of the hatched

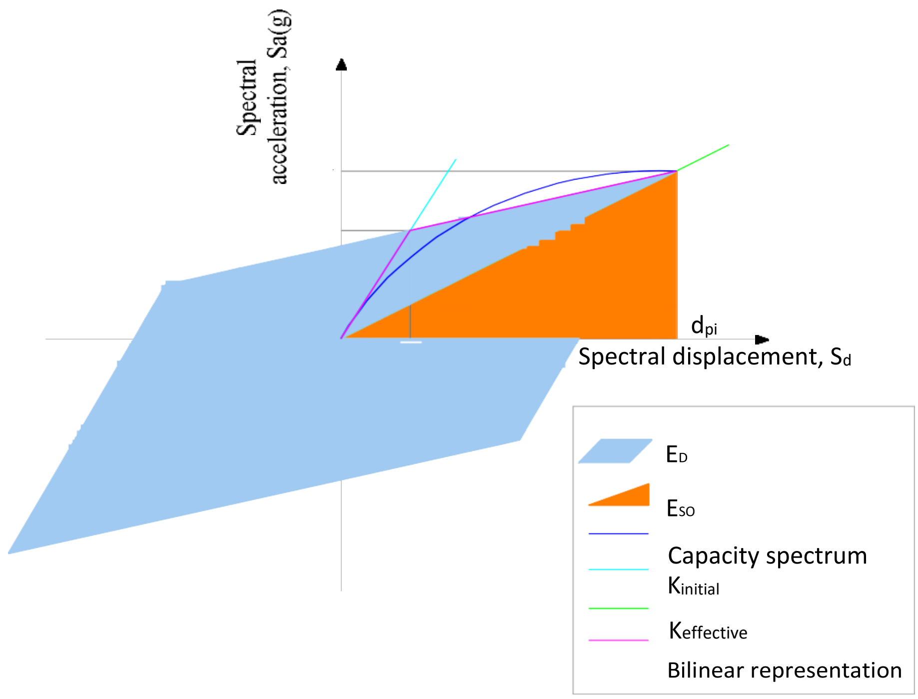


Fig 5

The ATC-40 proposes three categories of structural behavior, Types A, B, and C. The structural action of Type A is stable nature( full hysteresis loops ,k=1.0), Type B is assigned a k value of 2/3 and represents a moderate reduction of area. Type C represents poor hysteretic behavior with a lesser loop area ( k=2/3).

### 3.1.3 Performance Point

It the intersection of the Capacity spectrum with the demand curve on the ADRS plot. If performance point is present on the plot, it means that the structure has enough stiffness to stand against the demand posed by the lateral forces. As the structure yields, the damping of the structure increases which leads to dissipation of the energy in due to damping rather than in the form of the work done in the form of displacement. Because of this phenomenon, the demand imposed had lesser impact on the structure.

### 3.1.4 Displacement Coefficient Method FEMA 273, 356,440

**Newmark and Hall (1982)** and **Miranda (2000)** proposed a new procedures, in which coefficients are applied to calculate the target displacement. In the **FEMA-273,356 & 440** document, this procedure is used to characterize the displacement demand. This method mostly calculates the elastic displacement demand of an equivalent SDOF system, by assuming initial linear elastic properties and damping. In this method, the displacement demand is represented by reducing the elastic demand spectra (response spectrum) by the correction coefficients are $C_o$ , C1, $C_2$ , $C_3$ to the inelastic demand spectra (constant-ductility demand spectrum) which have better representation than elastic spectra, with equivalent viscous damping **(Fajfar 1999)**.

Following are the steps to be followed :

Post-elastic stiffness( $K_s$ )is calculated as shown in figure
The effective elastic stiffness, $K_e$ (at base shear $0.6V_b$ secant cut on the capacity cureve)
The effective fundamental period ($T_{eq}$) is found from Equation

$$\text{Teq} = Ti^2\sqrt{\frac{K_i}{K_o}} \quad \ldots\ldots\ldots\ldots\ldots\ldots\ldots\ldots\ldots\ldots\ldots\ldots\ldots 4$$

$T_i$ is the elastic fundamental period and $K_i$ represents the initial stiffness.

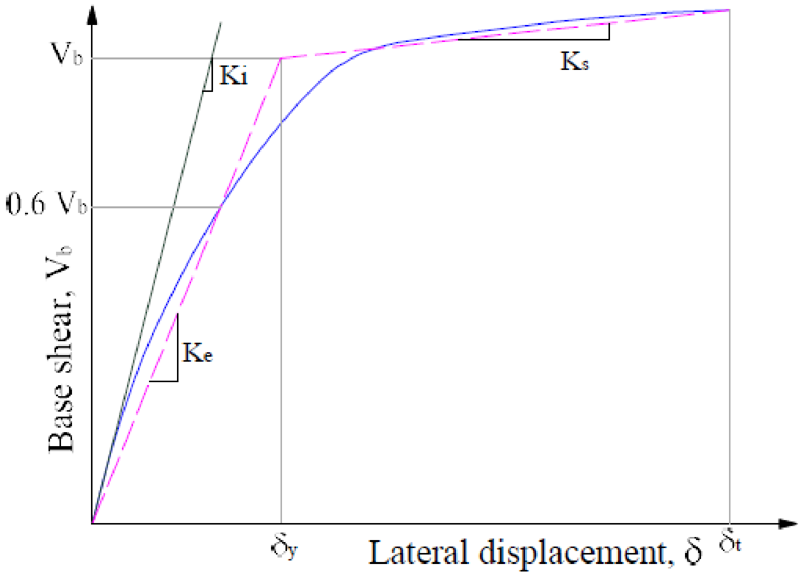


Fig 6 (Capacity Curve)

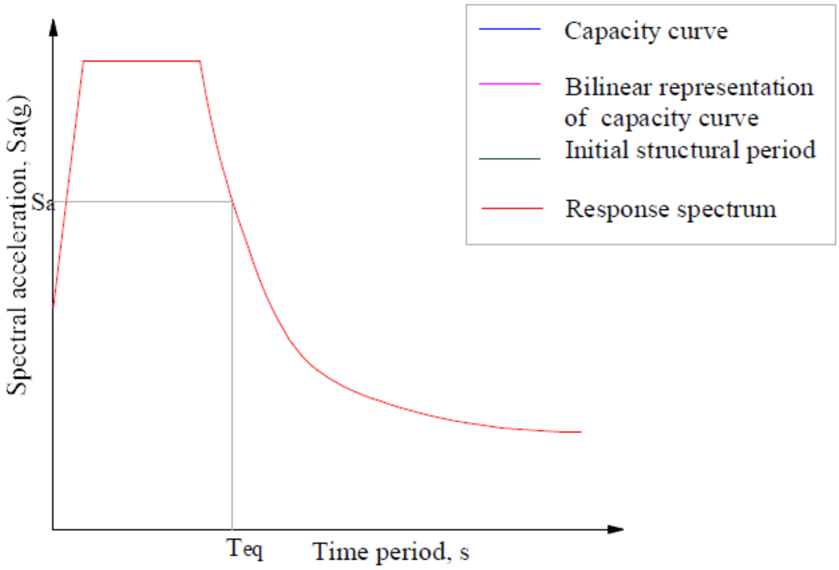


Fig 7 (Elastic response Spectrum)

The equivalent period is the time period of equivalent SDOF system which is linear. Sd is spectral displacement for the calculated effective time period of the equivalent SDOF

$$S_d = \frac{T_{eq}^2}{4\pi^2} \quad \ldots\ldots\ldots\ldots\ldots\ldots\ldots\ldots\ldots\ldots\ldots \quad 5$$

The expected maximum target displacement ( $\delta$t)

$$\delta t = C_o C_1 C_2 C_3 S_d \quad \ldots\ldots\ldots\ldots\ldots\ldots\ldots\ldots\ldots\ldots\ldots \quad 6$$

Substituting Sd

$$\delta t = C_o C_1 C_2 C_3 \frac{T_{eq}^2}{4\pi^2} \quad \ldots\ldots\ldots\ldots\ldots\ldots\ldots\ldots\ldots\ldots\ldots \quad 7$$

where,
$C_0$ = modification factor(relates spectral displacement to top displacement)
$C_1$ =modification factor relating expected maximum inelastic displacements to the displacements calculated for the linear elastic response.

$$C_1 = 1\, for\, T_{eq} \geq T_o \quad \ldots\ldots\ldots\ldots\ldots\ldots\ldots\ldots\ldots\ldots..8$$

$$= \frac{1+\left(R-1\right)\frac{T_o}{T_{eq}}}{R} \quad for\, T_{eq} < T_o$$

$C_1$ $can'tbe\ more\ than$ 2 $for\ T_{eq}$ < 0.1

$T_0$ is the characteristic period of the response spectrum, defined as time period associated with the transition from constant acceleration segment of the response spectrum to the constant velocity segment of the spectrum.

R is the ratio of the inelastic strength demand to calculate the yield strength coefficient as given in Equation

$$\mathrm{R} = \frac{\frac{S_a}{g}}{\frac{V_y}{W}} * \frac{1}{C_o} \quad \ldots\ldots\ldots\ldots\ldots\ldots\ldots\ldots\ldots\ldots\ldots\ldots \quad 9$$

$S_a$ is the response spectrum acceleration determined from the effective fundamental period of the structure.
$V_y$ is the Yield strength calculated using the capacity curve (a bilinear relation characterizes capacity curve)
W is the total dead load and anticipated live load
C2 - modification factor to represent the effect of the hysteresis shape on the maximum displacement response.
C3 - modification factor to represent the increased displacements due to second order effects.
$S_d$ is Spectral displacement

Chopra and Goel (1999) developed the capacity-demand-diagram method, using the constant-ductility demand spectrum, instead of the elastic design spectrum in the ATC-40. According to Chopra and Goel, the ATC-40 (1996) procedure significantly underestimates the deformation of inelastic systems for a wide range of Tn and ductility (μ) values, compared to the value determined from the inelastic design spectrum, using three different Ry- μ- Tn equations (Tn - natural period, Ry - yield strength reduction factor, μ- ductility), all of which provided similar results.

### 3.2 Plastic Hinges

The potential plastic hinge zones must be detailed carefully for the consideration of ductility to make sure that the shaking from a large earthquake displacement will not cause collapse. To boost the ductility, closely spaced hoops are provided in the potential plastic hinge location so that the longitudinal reinforcement doesn't buckle and the crushed concrete doesn't spall from the confined core. For a gravity load resisting element
There are two kinds of plastic hinges which can form in a structure named as reversing and non reversing depending on the magnitude of the gravity and lateral loads. If the gravity load dominates the lateral load (earthquake/wind) then negative moment hinges are formed at the column beam joint faces and positive moment hinges are formed in positive moment zones. The negative moment plastic hinges dissipate the energy by hysteretic behavior but positive moment hinges don't show any such behavior as the moment direction doesn't change because of high gravity loading. The positive moment plastic hinges are also known as **unidirectional** plastic hinges. In reversing plastic hinges, the tension and compression (compression reinforcements doesn't yield ultimately) reinforcements yields in each half cycles.
On the other hand, in case of non-reversing plastic hinges, only the tension reinforcements yield in both half cycles of the reversing actions. In reverse plastic hinges as compression reinforcements don't yield as much as tension reinforcements, makes tension reinforcements elongated which leads to opened cracks and slightly increases in the length of the beam. Because of this the concrete in plastic hinge zone disintegrates and the truss-like action of the stirrups resists all shear. The change in length is 2-4 % of the length of the beam. As the length of the beam increases, it starts to act like a catenary which induces axial forces in the beam. It causes slip of the main reinforcement in lapping zone. Hence if the beam is quite long and gravity dominated than it must be checked if there is any possibility of non-reversing plastic hinge formation.

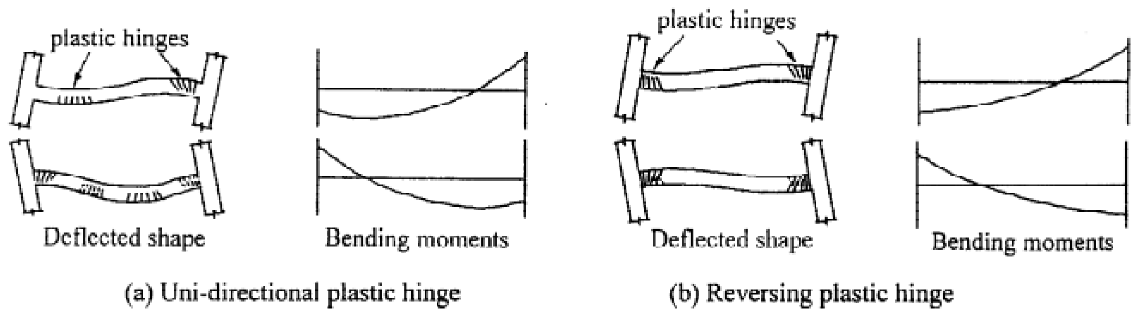


**Kim T. Douglas, Barry J. Davidson, Modelling of Reinforced Concrete Plastic Hinges**
Fig 8

From the above figure it is clear that in the central span of the beam moment direction doesn't change with reversing of the lateral force. On the other hand moments at the beam-column joint face changes direction in each half cycle.

### 3.3 Lumped Plasticity vs Distributed Plasticity

The inelastic behavious of the concrete can be modelled as Lumped, continuum and distributed. The continuum model is the most accurate and time consuming also.

#### 3.3.1 Lumped Plasticity

Lumped plasticity is also known as concentrated plasticity model. In this philosophy, the whole element is treated as elastic material except a particular location, which is known as a potential hinge location. The inelastic effect remains concentrated in this zone. This lumped plasticity model reduces the computational time significantly, although the results from the lumped plasticity are less accurate than the distributed flexibility.

#### 3.3.2 Fibre Hinges

In comparison to lumped plasticity, fiber hinges consider the material nonlinearity in the whole model. Hence the plastic hinges can form anywhere in the element, not only on the potential hinge locations. The fiber hinges give a little bit more realistic results. The mathematical model with fiber hinges is quite large and hence, takes a lot of computational effort to provide accurate results.

In this study, beams and columns are modeled as line elements, shear wall and slabs are modeled as shell elements. For beams and columns Lumped, plasticity is considered at the potential hinge locations. For area elements (shells), fiber hinges are considered.

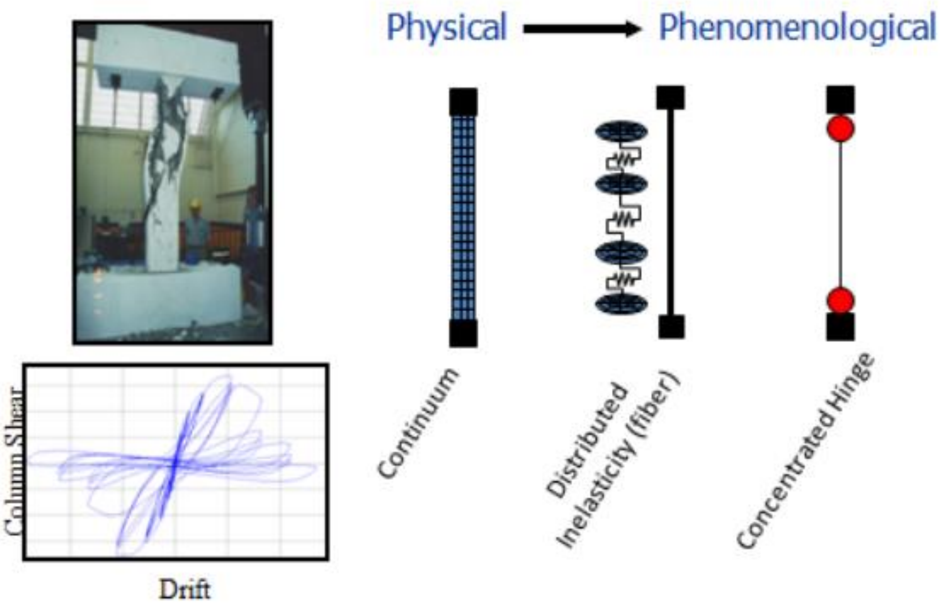


Fig 9 (ATC 72-1)

## 3.4 Acceptability Criterion

There is two criteria are considered. For element level code provisions from FEMA 356 and ASCE 41-13 are considered. For structural level, the acceptability criterion is taken from the target performance defined by the client.

### 3.4.1 Element Acceptance Criterion

Element acceptance criterion is taken from ASCE 41-13.

| | | | ACCEPTANCE CRITERIA | | |
|---|---|---|---|---|---|
| | | | PLASTIC ROTATIONS | | |
| | | | PERFORMANCE LEVELS | | |
| | | | IO | LS | *CP* |
| Beams controlled by flexure | | | | | |
| $\frac{\rho - \rho'}{\rho_{bal}}$ | Transverse Reinforcements | $\frac{V}{b_w d\sqrt{f'_c}}$ | | | |
| <=0.0 | C | <=3 (0.25) | 0.010 | 0.025 | 0.05 |
| <=0.0 | C | >=6(0.5) | 0.005 | 0.02 | 0.04 |
| >=0.5 | C | <=3 (0.25) | 0.005 | 0.02 | 0.03 |
| >=0.5 | C | >=6(0.5) | 0.005 | 0.015 | 0.02 |
| <=0.0 | NC | <=3 (0.25) | 0.005 | 0.02 | 0.03 |
| <=0.0 | NC | >=6 (0.5) | 0.0015 | 0.010 | 0.015 |
| >=0.5 | NC | <=3 (0.25) | 0.005 | 0.01 | 0.015 |
| >=0.5 | NC | >=6 (0.5) | 0.0015 | 0.005 | 0.01 |

**TABLE 3**
**ACCEPTANCE CRITERIA FOR BEAMS TABLE**

| | | | Acceptance Criteria | | |
|---|---|---|---|---|---|
| | | | Plastic Rotation Angle | | |
| | | | Performance Level | | |
| | | | IO | LS | CP |
| $\frac{P}{A_g f'}$ | $\rho = \frac{A_v}{b_w s}$ | | 0.005 | 0.045 | 0.060 |
| <=0. | >=.006 | | 0.005 | 0.045 | 0.06 |
| >=0.6 | >=0.006 | | 0.003 | 0.009 | 0.01 |
| <=0.1 | =0.002 | | 0.005 | 0.027 | 0.034 |
| >=0.6 | =0.002 | | 0.002 | 0.004 | 0.0035 |
| $\frac{P}{A_g f'_c}$ | $\rho = \frac{A_v}{b_w s}$ | $\frac{V}{b_w d\sqrt{f'_c}}$ | | | |
| <=0.1 | >=0.006 | <=3 (0.25) | 0.005 | 0.045 | 0.06 |
| <=0.1 | >=0.006 | >=6 (0.5) | 0.005 | 0.045 | 0.06 |
| >=0.6 | >=0.006 | <=3 (0.25) | 0.003 | 0.009 | 0.01 |
| >=0.6 | >=0.006 | >=6(0.5) | 0.003 | 0.007 | 0.008 |

**TABLE 4**
**Acceptance Criteria For Columns (Non Linear Procedures)**

### 3.4.2 Acceptability Criteria for Structure as a Whole

Acceptable damage for a structure depends on the purpose of the structure. For example, for a building which is constructed for rent purpose, it is necessary to design in such a way that under the design level earthquake, not more than a certain limit of floor area is damaged. This limit is defined by the client. For the study purpose, in the project it is defined as under design threat, not more than 10% floor area of at a story level be beyond **Life Safety** limit state.
The traditional problem encountered with Indian Standards is that the standards only consider the structural element damage. Indian codes don’t take care about the non-structural elements. The threat posed by earthquake against non-structural elements is huge, as the value of non-structural elements if not equal than isn’t less than structural elements. Essential non-structural elements are electronic equipment, pipe fittings, electrical fittings, and wires. If these non-structural elements are damages than structure wouldn’t be serviceable. For example, a situation can be considered for a hospital. If during the earthquake the response acceleration of the floor is high, then medical equipment can get damaged which can cost life to a patient.

### 3.4.3 Non Structural Component Acceptance Criteria

The poor performance of non-structural elements can lead to damage, loss or business interruption. Natural philosophy of design gives more importance to the design of structural elements neglecting the importance of the performance of non-structural elements. Following are some main non-structural elements:

Architectural Components

- Cladding
- Partition walls
- Racks and shelves
- Ceilings

Equipment

- Electrical power backup
- Heating and Ventilation system
- Fire Protection System
- Computers and Medical Equipment

Building Contents

- Storage
- Production Equipment
- Supplies/Inventory

For particular cases, the value of non-structural elements can be far more than the net worth of the building. For example, if machines stop functioning due to earthquake motion, it can lead to business loss. Such a situation can cause a slump in the share market and may also affect the brand image of the company. Non structural damage may lead to Loss of operation, Loss of service, Loss of market share, and business continuity.

There are two types of non-structural elements

- Inertial Failure

- Displacement Failure

Inertial failures are caused by excessive shaking/ rocking of the equipment due to unanchored condition. A component may also slide or overturn due to high response acceleration of the building. For bridges, high acceleration may cause overturn or collision of the vehicles.
Deformation failures are caused by excessive building drifts and interaction between structural and non-structural elements.
The non-structural elements damage can be controlled by limiting the story drifts and response accelerations of the floors.

### 3.5 Acceptance Criteria for Model

Following limits are considered for the acceptance criteria for the building. These limits include rotation angles for beams and columns given in the following table

| | Acceptance criteria: Plastic rotation anagle in radians | | |
|---|---|---|---|
| | Performance Level | | |
| | Immediate Occupancy | Life Safety | Collapse Prevention |
| BEAMS | | | |
| Low Shear, well confined | 0.5-1 | 1-2 | 2-2.5 |
| High shear, well confined | 0.5 | 0.5-1 | 1.5-2 |
| Low Shear, Poorly Confined | 0.5 | 1 | 1-2 |
| High Shear, Poorly Confined | 0.15 | 0.5 | 0.5-1 |
| Columns | | | |
| Low axial load, well confined | 0.5 | 1.2-1.5 | 1.6-2 |
| High axial load, well confined | 0.3 | 1-1.2 | 1.2-1.5 |
| Low axial load, poorly confined | 0.5 | 0.4-0.5 | 0.5-0.6 |
| High axial load, poorly confined | 0.2 | 0.2 | 0.2-0.3 |

Table 5

Table Structural Performance Criteria

| Performance Level | Storey drift | | |
|---|---|---|---|
| | No Damage | Repairable damage | No collapse |
| Buildings with brittle non-structural elements | 0.4% | 2.5% | No limit |
| Buildings with ductile non-structural elements | 0.7% | 2.5% | No limit |
| Buildings with non-structural elements designed to sustain buildings displacements | 1% | 2.5% | No limit |

Table 6

Table Nonstructural Performance Level

| Performance Level | Limiting strain in Plastic hinges | | |
|---|---|---|---|
| | No Damage | Repairable damage | No Collapse |
| Concrete Compressive strain | 0.4% | $0.4\%+1.4p_v f_{yh}(e_{su})_t/(f'_{cc})^{a,b}$ | 1.5 times repairable damage limit |
| Longitudinal reinforcement tensile strain | 1.5% | $0.6(e_{su})_l$ or 5% if less | 1.5 times repairable damage limit |
| Structural steel strain, flexural plastic hinges | 1% | No limit | No limit |

Table 7

Structural Performance Level Limiting Strains

# CHAPTER 4.
# MODELING

## 4.1 Modelling Concrete for Non-Linear Analysis

An equivalent envelope curve can model the hysteresis curve for cyclic loading. This envelope curve can be used for replacing the hysteresis for cyclically loaded elements.

The properties of the concrete at near collapse stage are quite different from those considered for linear analysis and design. Non-Linear behavior of the concrete includes crushing, cracking, tension stiffening, compression softening, and bond slip. Stiffness degradation and **Bausschinger** effect in reinforcing steel make concrete expression more complex. To model the nonlinear effects for the concrete, there are mainly three methods

- Based on the theory of elasticity
- Based on the theory of plasticity
- Based on the theory of Fracture Mechanics

The models based on the theory of plasticity and fracture mechanics are very complex as they include multiple parameters which it nearly impossible to create a mathematical model. Very deep research is done by **Sinha et al.**, **Karsan and Mander**, **Bahn and Hsu**, **Elmorsi et al.**, **Palermo and Vecchio**, **Mansour and Hsu and Sima et al.** for nonlinear modeling effects in concrete.

**Sinha** was the first one to model the concrete as a nonlinear material. He conducted tests on 48 cylinders with 20 to 28 Mpa compressive strength under reverse cyclic axial loading and derived a stress-strain concrete.
After Sinha, **Karsan and Jirsa** further conducted tests on the previous work of Sinha. They experimented the effect of reverse cyclic lateral load on various combinations of axial compressive loads on Plain Cement concrete 46 short rectangular columns. They found that there exists an envelope curve that can be represented by a monotonic curve as the response of the same concrete properties as per their residual plastic strain as the main parameter to determine the unloading curve equation. If the reloading starts from zero stress condition, as the curve progress in meeting envelope, it becomes flatter and could be represented as a straight line.

**Manders** model is the most widely used model. Other models did not consider the effect of the rate of change of the strain. Menders model included this effect, which made the experiment as the most precise model to a real earthquake situation.

### 4.2 Envelope Curve under Different Loading Conditions

The slope at the beginning of the curve is equal to the initial modulus of the elasticity of the concrete. When a concrete element is monotonically loaded under compressive load to a strain level and then released to zero stress condition, it's observed from the experiments that the unloading curves are concave from the unloading point. Initially, the stiffness is high gradually reduces to zero under unloading condition. In the release stage, the plastic strains are quite high. From experiments, it pointed out under reloading stage the curve is flatter than the previous loading, which shows the damage accumulation and stiffness degradation.

**Reinhardt and Reinhardt et al.** conducted more than 100 test under cyclic tension loading on the concrete specimens. They observed that the reloading curve does not return to the envelope curve at the previous maximum point. More strain needed to reach the last location on the envelope curve. In comparison with compression loading case, there is negligible energy dissipation in the case of the tension cyclic loading case.

**Ramatani et al.** attempted to characterize the effect tension when the element is loaded under cyclic compressive loads. The test results indicated that once a crack is formed due to tensile stress, to close the crack completely compression is required. Once the crack is closed completely, the stiffness of concrete is not affected by the accumulated damage due to the tension.

### 4.3 Mander Concrete Model

Mander developed a stress-strain curve of confined as well as unconfined concrete under uniaxial compressive loading. Mander considered both types of confining be it rectangular hoops or circular hoops. Mader's model includes the cyclic loading as well as strain rate effect. Energy balance method is used to characterize the longitudinal compressive strain in concrete at the first fracture of confinement reinforcement by equating accumulated strain energy capacity to strain energy stored in concrete.

#### 4.3.1 Unified Stress-Strain Approach for Confined Concrete with Monotonic Loading at slow Strain Rates

Mander proposed stress-strain for confined concrete applicable to circular as well as rectangular hoops in the form of transverse reinforcement. For a slow strain rate and monotonic loading, compressive stress is given by

$$f_c = \frac{f'_{cc} x r}{r-1+x^r} \quad \ldots\ldots\ldots\ldots\ldots\ldots\ldots\ldots\ldots\ldots \; 10$$

Where f’cc= compressive strength of the confined concrete

$$X = \frac{\epsilon_c}{\epsilon_{cc}} \quad \ldots\ldots\ldots\ldots\ldots\ldots\ldots\ldots\ldots\ldots\ldots\ldots 11$$

Where ∈c = longitudinal compressive concrete strain

$$\in cc = \in co\left[1 + 5\left(\frac{f'cc}{f'co} - 1\right)\right] \ldots\ldots 12$$

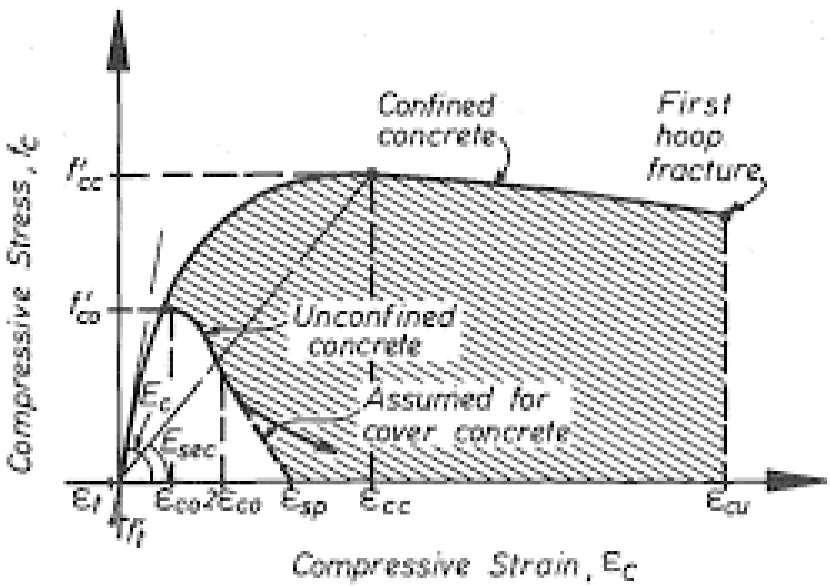


Fig 10 (Manders Model )

$$r = \frac{Ec}{Ec - Esec} \ldots\ldots 13$$

$$Ec = 5000\sqrt{f'co}$$

Ec is the tangent modulus of elasticity of the concrete (MPa)

$$E_{sec} = \frac{f'cc}{\epsilon cc} \ldots\ldots 14$$

### 4.3.2Effective Lateral Confining Pressure and the Confinement

The maximum confining pressure due to the stirrups is effective only on the core part of the concrete due to the arching action of the concrete.

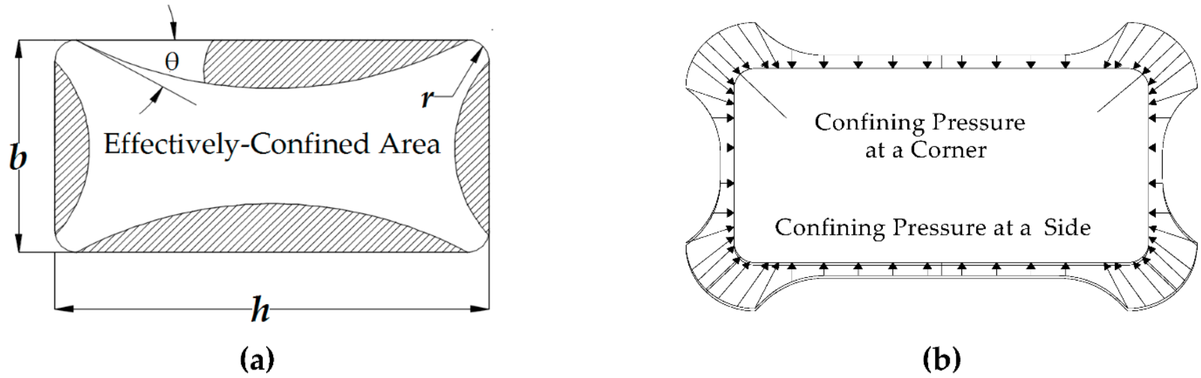


Fig 11
( https://www.mdpi.com/2073-4360/8/9/323)

The effective lateral confining pressure is given by the following equation

$$f'_{cc} = f_1 k_e \quad \ldots\ldots\ldots\ldots\ldots\ldots\ldots\ldots\ldots\ldots\ldots\ldots 15$$

where f1 = confining pressure from the stirrups (uniformly distributed over the core)

$$ke = \frac{A_e}{A_{cc}} \quad \ldots\ldots\ldots\ldots\ldots\ldots\ldots\ldots\ldots\ldots\ldots\ldots\ldots 16$$

=confinement effectiveness coefficient
Ae= area of confined core (effectively)
Acc = Ac (1 - $\rho cc$)
$\rho cc$ = area of longitudinal reinforcement / area of core section

## 4.4 PUSHOVER ANALYSIS

A structure consisting of 17 stories with Height of 52 meters is considered. On these different types of Pushover analysis and NonLinear time, history analysis is done. In last the comparison of the different kinds of Pushover analysis are compared with Non-Linear time History analysis are examined, as Non-Linear Time History analysis is the most credible analysis which gives the best prediction of the real model. The Pushover analysis, which offers the best results will be implemented on the other structures.

First, the structure is 38nalysed for the linear load cases. Following load pattern are considered for the linear analysis:

- Dead Load
- Live Load
- Wind Load
- Earthquake Load
- Response Spectrum

After analysis, the following checks are applied to the structure:
Lateral Drift Under Service Loads
Lateral Deflection
Check for the weak story
Check for soft story
Check for Vertical and Horizontal Irregularity
Check for Weak Column and strong beam

The structure is designed after analysis and the following checks are applies as per Indian standards.

Following types of Pushover analysis are considered
Pushover Analysis
Modal Pushover Analysis
Modal combination Analysis

Following are the results for modal analysis:

| Case | Mode | Period | UX | UY | RZ | Sum RZ |
|---|---|---|---|---|---|---|
| Modal | 1 | 2.523 | 0.1653 | 0.4956 | 0.0902 | 0.0902 |
| Modal | 2 | 2.431 | 0.5111 | 0.2063 | 0.0136 | 0.1038 |
| Modal | 3 | 1.819 | 0.0547 | 0.0306 | 0.608 | 0.7118 |
| Modal | 4 | 1.169 | 0.015 | 0.1291 | 0.024 | 0.7359 |
| Modal | 5 | 1.133 | 0.1367 | 0.0223 | 0.0063 | 0.7421 |
| Modal | 6 | 1.021 | 0.01 | 0.0076 | 0.1379 | 0.8801 |
| Modal | 7 | 0.574 | 0.000006569 | 0.0454 | 0.0002 | 0.8803 |
| Modal | 8 | 0.56 | 0.0443 | 0.0001 | 0.0007 | 0.8809 |
| Modal | 9 | 0.48 | 0.0036 | 0.0021 | 0.056 | 0.9369 |
| Modal | 10 | 0.433 | 0.0002 | 0.0222 | 0.000009727 | 0.9369 |
| Modal | 11 | 0.422 | 0.0217 | 0.000002508 | 0.00002402 | 0.937 |
| Modal | 12 | 0.382 | 0.0002 | 0.0003 | 0.0204 | 0.9574 |

Table 8
Modal Time Period & Mass Participation Ratios

Following are the observations from the above table

- First two modes are translational
- Third mode it rotational
- First and Fourth modes are in the Y direction while second and fifth modes are in the X direction
- Hence First and Fourth modes are the First and Second principal modes of the Y direction. While second and Fifth modes are the First and second modes in X principal direction.

Pictures on the next page depict the modes shapes. Forces are computed from these modes for the modal combination Pushover analysis. Following three types of Pushover analysis are considered

Pushover (based on triangular lateral load pattern)

Modal Pushover Analysis (Lateral Load pattern in shape of a particular mode)

Modal Combination Pushover analysis (Pushover analysis based on a combination of different mode shapes).

## 4.5 Selection and Scaling of Time Histories

For nonlinear time history analysis, five time histories were selected and matched to the response spectrum defined as per IS 1893 (2016) in the time domain. Following is the list of selected time histories:

| Earthquake | Peak ground Acceleration |
|---|---|
| El Centro 1940 | 3.425 $m/s^2$ (0.34g) |
| Chamoli 1999 | 3.52 $m/s^2$ (0.352g) |
| Uttarkashi 1991 | 3.04 $m/s^2$ (0.304g) |

Table 9

All the time, histories are collected from https://strongmotioncenter.org.

The time histories of Kobe and El Centro earthquakes are matched with the response spectrum mentioned in IS 1893. For design basis earthquake, the structure is analyzed for Bhuj earthquake time history and scaled time histories of other earthquakes in so that the peak acceleration of the earthquake becomes 0.18g.

For Maximum considered earthquake, the time histories are scaled so that the peak ground acceleration is not less than 0.36g.

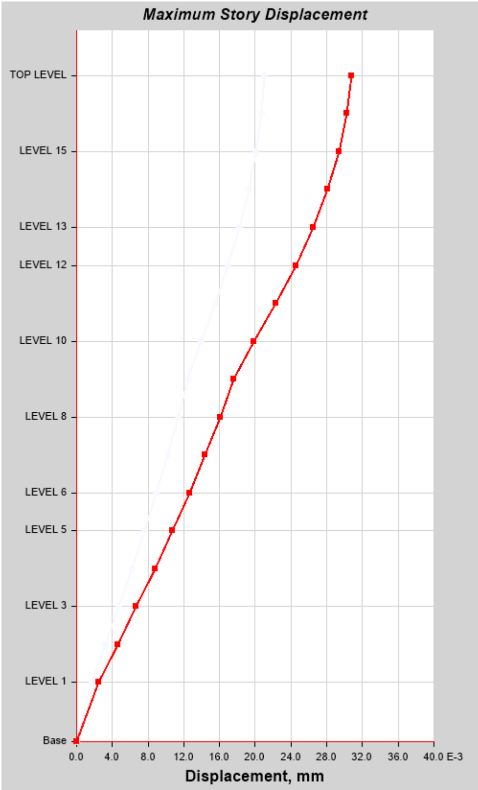


Mode 1

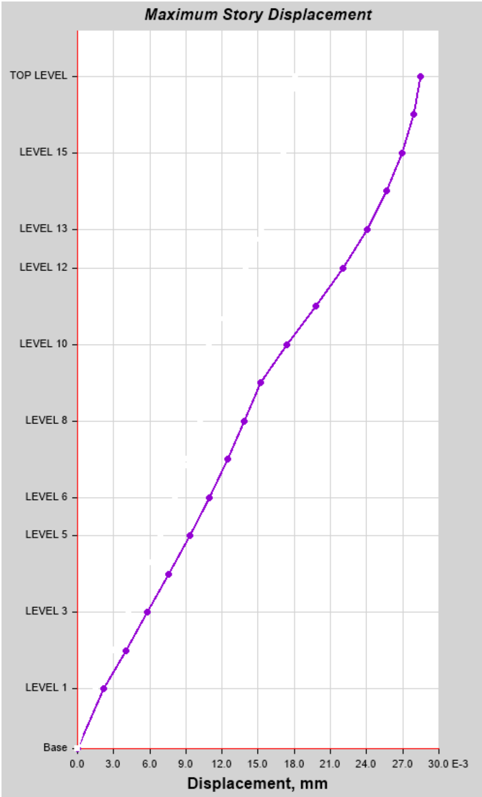


Mode 2

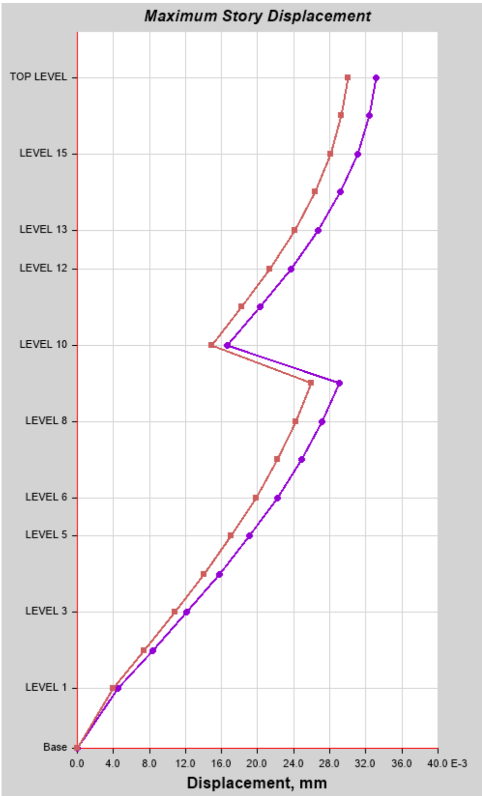


Mode 3

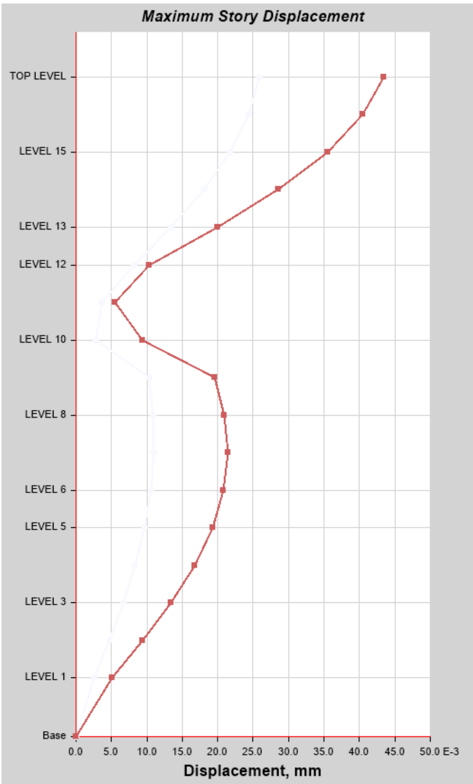


Mode 4

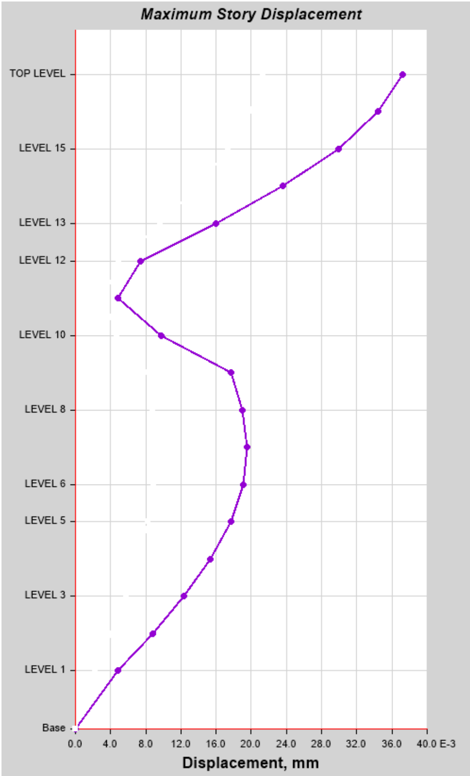


Mode 5

Following is a table showing the mode shapes under different modes of vibrations

| Story | Mode1 | | Mode 2 | | Mode 3 | | Mode 4 | | Mode 5 | |
|---|---|---|---|---|---|---|---|---|---|---|
| | X | Y | X | Y | X | Y | x | y | X | Y |
| 17 | 21.003 | 30.74 | 28.421 | 17.737 | 32.837 | 29.71 | 23.259 | 42.985 | 38.099 | 19.787 |
| 16 | 20.646 | 30.209 | 27.861 | 17.402 | 32.1 | 29.039 | 21.938 | 40.134 | 35.361 | 18.51 |
| 15 | 20.007 | 29.332 | 26.971 | 16.852 | 30.82 | 27.868 | 19.666 | 35.305 | 30.841 | 16.338 |
| 14 | 19.262 | 28.086 | 25.722 | 16.067 | 28.957 | 26.161 | 16.441 | 28.521 | 24.581 | 13.279 |
| 13 | 18.228 | 26.48 | 24.12 | 15.049 | 26.531 | 23.936 | 12.396 | 20.102 | 16.888 | 9.477 |
| 12 | 16.983 | 24.539 | 22.181 | 13.809 | 23.584 | 21.232 | 7.727 | 10.515 | 8.197 | 5.142 |
| 11 | 15.548 | 22.303 | 19.944 | 12.375 | 20.197 | 18.127 | 3.397 | 5.313 | 4.782 | 3.05 |
| 10 | 13.975 | 19.868 | 17.517 | 10.822 | 16.595 | 14.83 | 2.199 | 9.324 | 9.623 | 3.864 |
| 9 | 12.471 | 17.611 | 15.355 | 11.157 | 29.116 | 25.918 | 8.756 | 18.954 | 17.592 | 7.011 |
| 8 | 11.348 | 16.052 | 14.054 | 10.246 | 27.225 | 24.244 | 9.164 | 27.4 | 18.951 | 7.614 |
| 7 | 10.167 | 14.402 | 12.664 | 9.241 | 24.98 | 22.266 | 9.215 | 20.904 | 19.505 | 7.844 |
| 6 | 8.909 | 12.631 | 11.156 | 8.147 | 22.347 | 19.933 | 8.873 | 20.423 | 19.101 | 7.707 |
| 5 | 7.575 | 10.743 | 9.528 | 6.961 | 19.331 | 17.251 | 8.14 | 18.945 | 17.762 | 7.177 |
| 4 | 6.178 | 8.754 | 7.795 | 5.693 | 15.972 | 14.257 | 7.042 | 16.527 | 15.539 | 6.279 |
| 3 | 4.73 | 6.686 | 5.978 | 4.357 | 12.329 | 11.004 | 5.625 | 13.279 | 12.536 | 5.055 |
| 2 | 3.25 | 4.57 | 4.102 | 2.978 | 8.482 | 7.564 | 3.958 | 9.379 | 8.91 | 3.575 |
| 1 | 1.76 | 2.45 | 2.21 | 1.589 | 4.553 | 4.052 | 2.148 | 5.0943 | 4.889 | 1.942 |

Table 10

Following table shows the calculated forces in X and Y directions for different modes of vibrations

| Mode 1 | | Mode 2 | | Mode 3 | | Mode 4 | | Mode 5 | |
|---|---|---|---|---|---|---|---|---|---|
| X | Y | X | Y | X | Y | X | Y | X | Y |
| 47971.6 | 210506.3 | 208308.8 | 52473.71 | 34424.32 | 17423.63 | 10404.35 | 165491.6 | 160250.5 | 13576.95 |
| 47156.2 | 206870.1 | 204204.3 | 51482.64 | 33651.7 | 17030.12 | 9813.435 | 154515.3 | 148734 | 12700.73 |
| 45696.7 | 200864.4 | 197681.2 | 49855.5 | 32309.82 | 16343.38 | 8797.111 | 135923.7 | 129722.2 | 11210.4 |
| 43995.1 | 192331.9 | 188526.8 | 47533.13 | 30356.77 | 15342.3 | 7354.485 | 109805.4 | 103391.6 | 9111.451 |
| 41633.4 | 181334 | 176785.1 | 44521.44 | 27813.49 | 14037.43 | 5545.052 | 77392.39 | 71033.63 | 6502.69 |
| 38789.78 | 168042.1 | 162573.4 | 40852.99 | 24724.04 | 12451.65 | 3456.487 | 40482.59 | 34477.89 | 3528.208 |
| 35512.19 | 152730.1 | 146177.5 | 36610.6 | 21173.31 | 10630.7 | 1519.566 | 20454.97 | 20113.86 | 2092.772 |
| 31919.4 | 136055.3 | 128389.1 | 32016.15 | 17397.19 | 8697.154 | 983.6696 | 35897.26 | 40475.88 | 2651.302 |
| 88526.7 | 374813.7 | 349774.5 | 102583.9 | 94864.5 | 47239.75 | 12173.06 | 226793.2 | 229970 | 14951.07 |
| 57938.87 | 245718.7 | 230258.7 | 67758.5 | 63799.55 | 31782.5 | 9163.405 | 235807.4 | 178182.8 | 11678.39 |
| 51909.1 | 220461.1 | 207485.1 | 61112.26 | 58538.58 | 29189.46 | 9214.402 | 179902.1 | 183391.6 | 12031.16 |
| 45486.2 | 193351.2 | 182778.3 | 53877.46 | 52368.36 | 26131.03 | 8872.424 | 175762.5 | 179593.1 | 11821.03 |
| 38675.27 | 164450.3 | 156105.4 | 46034.25 | 45300.61 | 22615.08 | 8139.472 | 163042.7 | 167003.5 | 11008.11 |
| 31542.68 | 134003.4 | 127712.1 | 37648.75 | 37429.07 | 18690.11 | 7041.543 | 142233.1 | 146102.2 | 9630.757 |
| 24149.7 | 102347.1 | 97942.68 | 28813.56 | 28892 | 14425.62 | 5624.635 | 114280.5 | 117867.1 | 7753.381 |
| 16593.35 | 69956.06 | 67206.57 | 19694.01 | 19876.87 | 9915.973 | 3957.743 | 80716.69 | 83774.4 | 5483.35 |
| 8985.937 | 37503.79 | 36208.32 | 10508.32 | 10669.58 | 5311.941 | 2147.861 | 43842.1 | 45967.79 | 2978.648 |

Table 11
Lateral Forces (KN)

Different modes are combined as per mass participation ratios under different modes to calculate the final forces. The first five modes of vibrations give 85% of the mass participation ratio. The third mode is the torsional mode of vibration. Hence force corresponding to this mode will be a torque. In this study, torque as an action is ignored.

| Story | X | | | | | | | |
|---|---|---|---|---|---|---|---|---|
| | Mode(1+2+5) | Mode(1+2-5) | Mode(1-2+5) | Mode(1-2-5) | Mode(-1+2+5) | Mode(-1+2-5) | Mode(-1-2+5) | Mode(-1-2-5) |
| 17 | 416530.895 | 96029.9029 | -86.6991616 | -320587.691 | 320587.6913 | 86.69916161 | -96029.90294 | -416530.895 |
| 16 | 400094.565 | 102626.506 | -8314.10402 | -305782.163 | 305782.1631 | 8314.104017 | -102626.5063 | -400094.565 |
| 15 | 373100.059 | 113655.688 | -22262.2833 | -281706.654 | 281706.6545 | 22262.28328 | -113655.6879 | -373100.059 |
| 14 | 335913.473 | 129130.227 | -41140.0354 | -247923.281 | 247923.2814 | 41140.03543 | -129130.2269 | -335913.473 |
| 13 | 289452.096 | 147384.83 | -64118.0242 | -206185.29 | 206185.2899 | 64118.02421 | -147384.8298 | -289452.096 |
| 12 | 235841.032 | 166885.242 | -89305.6855 | -158261.475 | 158261.4752 | 89305.68552 | -166885.2422 | -235841.032 |
| 11 | 201803.542 | 161575.826 | -90551.4522 | -130779.168 | 130779.168 | 90551.45223 | -161575.8265 | -201803.542 |
| 10 | 200784.329 | 119832.57 | -55993.7721 | -136945.531 | 136945.5306 | 55993.7721 | -119832.57 | -200784.329 |
| 9 | 668271.193 | 208331.259 | -31277.8614 | -491217.795 | 491217.7954 | 31277.86139 | -208331.2586 | -668271.193 |
| 8 | 466380.326 | 110014.763 | 5862.97478 | -350502.588 | 350502.5881 | -5862.97478 | -110014.7629 | -466380.326 |
| 7 | 442785.87 | 76002.5708 | 27815.6314 | -338967.668 | 338967.6678 | -27815.6314 | -76002.57081 | -442785.87 |
| 6 | 407857.592 | 48671.3423 | 42301.0551 | -316885.194 | 316885.1945 | -42301.0551 | -48671.34226 | -407857.592 |
| 5 | 361784.082 | 27777.1626 | 49573.3717 | -284433.548 | 284433.5476 | -49573.3717 | -27777.16257 | -361784.082 |
| 4 | 305356.988 | 13152.6462 | 49932.7137 | -242271.628 | 242271.6281 | -49932.7137 | -13152.64618 | -305356.988 |
| 3 | 239959.477 | 4225.28369 | 44074.1258 | -191660.067 | 191660.0674 | -44074.1258 | -4225.283694 | -239959.477 |
| 2 | 167574.312 | 25.5193251 | 33161.1786 | -134387.614 | 134387.6139 | -33161.1786 | -25.51932512 | -167574.312 |
| 1 | 91162.0442 | -773.538947 | 18745.4123 | -73190.1709 | 73190.17092 | -18745.4123 | 773.5389475 | -91162.0442 |
| Force in X direction Under different modal combinations | | | | | | | | |

Table 12

| Story | Y | | | | | | | |
|---|---|---|---|---|---|---|---|---|
| | Mode(1+2+4) | Mode(1+2-4) | Mode(1-2+4) | Mode(1-2-4) | Mode(-1+2+4) | Mode(-1+2-4) | Mode(-1-2+4) | Mode(-1-2-4) |
| 17 | 428471.6484 | 97488.46625 | 323524.2287 | -7458.953433 | 7458.953433 | -323524.2287 | -97488.46625 | -428471.6484 |
| 16 | 412867.9996 | 103837.4301 | 309902.7294 | 872.1598645 | -872.1598645 | -309902.7294 | -103837.4301 | -412867.9996 |
| 15 | 386643.6234 | 114796.2058 | 286932.6285 | 15085.21093 | -15085.21093 | -286932.6285 | -114796.2058 | -386643.6234 |
| 14 | 349670.3977 | 130059.5722 | 254604.1412 | 34993.31565 | -34993.31565 | -254604.1412 | -130059.5722 | -349670.3977 |
| 13 | 303247.8662 | 148463.0825 | 214204.9774 | 59420.19371 | -59420.19371 | -214204.9774 | -148463.0825 | -303247.8662 |
| 12 | 249377.7134 | 168412.5358 | 167671.7362 | 86706.55856 | -86706.55856 | -167671.7362 | -168412.5358 | -249377.7134 |
| 11 | 209795.6589 | 168885.7217 | 136574.4648 | 95664.52771 | -95664.52771 | -136574.4648 | -168885.7217 | -209795.6589 |
| 10 | 203968.7152 | 132174.2011 | 139936.4112 | 68141.8971 | -68141.8971 | -139936.4112 | -132174.2011 | -203968.7152 |
| 9 | 704190.7516 | 250604.4054 | 499022.984 | 45436.63781 | -45436.63781 | -499022.984 | -250604.4054 | -704190.7516 |
| 8 | 549284.5972 | 77669.87346 | 413767.6071 | -57847.11663 | 57847.11663 | -413767.6071 | -77669.87346 | -549284.5972 |
| 7 | 461475.4299 | 101671.2625 | 339250.9027 | -20553.26467 | 20553.26467 | -339250.9027 | -101671.2625 | -461475.4299 |
| 6 | 422991.2027 | 71466.11136 | 315236.2819 | -36288.80942 | 36288.80942 | -315236.2819 | -71466.11136 | -422991.2027 |
| 5 | 373527.277 | 47441.84121 | 281458.7851 | -44626.65069 | 44626.65069 | -281458.7851 | -47441.84121 | -373527.277 |
| 4 | 313885.2553 | 29418.95828 | 238587.7515 | -45878.54558 | 45878.54558 | -238587.7515 | -29418.95828 | -313885.2553 |
| 3 | 245441.1626 | 16880.14378 | 187814.0373 | -40746.98152 | 40746.98152 | -187814.0373 | -16880.14378 | -245441.1626 |
| 2 | 170366.7531 | 8933.377406 | 130978.7386 | -30454.63709 | 30454.63709 | -130978.7386 | -8933.377406 | -170366.7531 |
| 1 | 91854.21144 | 4170.018479 | 70837.57107 | -16846.62189 | 16846.62189 | -70837.57107 | -4170.018479 | -91854.21144 |
| Force in Y direction under different Modal Combinations | | | | | | | | |

Table 13

For the Modal Pushover combination analysis, the different mode shapes are combined depending on the mass participation ratio of the structure under different modes and the mass at the corresponding story level. The equation proposed by **Erol KALKAN and Shashi K. KUNNATH** is used to combine modes for calculating the lateral forces at different story levels.

$$F_j = \sum \mathrm{T}_n m \phi_n S_a \ldots\ldots\ldots\ldots\ldots\ldots\ldots\ldots\ldots\ldots\ldots\ldots 17$$

Where T $= modal\ mass\ participation\ ratio\ in\ mode\ n$

M= mass at the story i

$\phi n = mode\ shape\ for\ the\ mode\ n$

$S_a$ = spectral acceleration at the period corresponding to mode n

### 4.6 Following pictures shows lateral load pattern for Modal Combination Pushover in the X direction

These lateral load patterns are derived from a combination of the individual modes. The first five modes are considered because they make it up to 85 % of the modal mass participation ratio

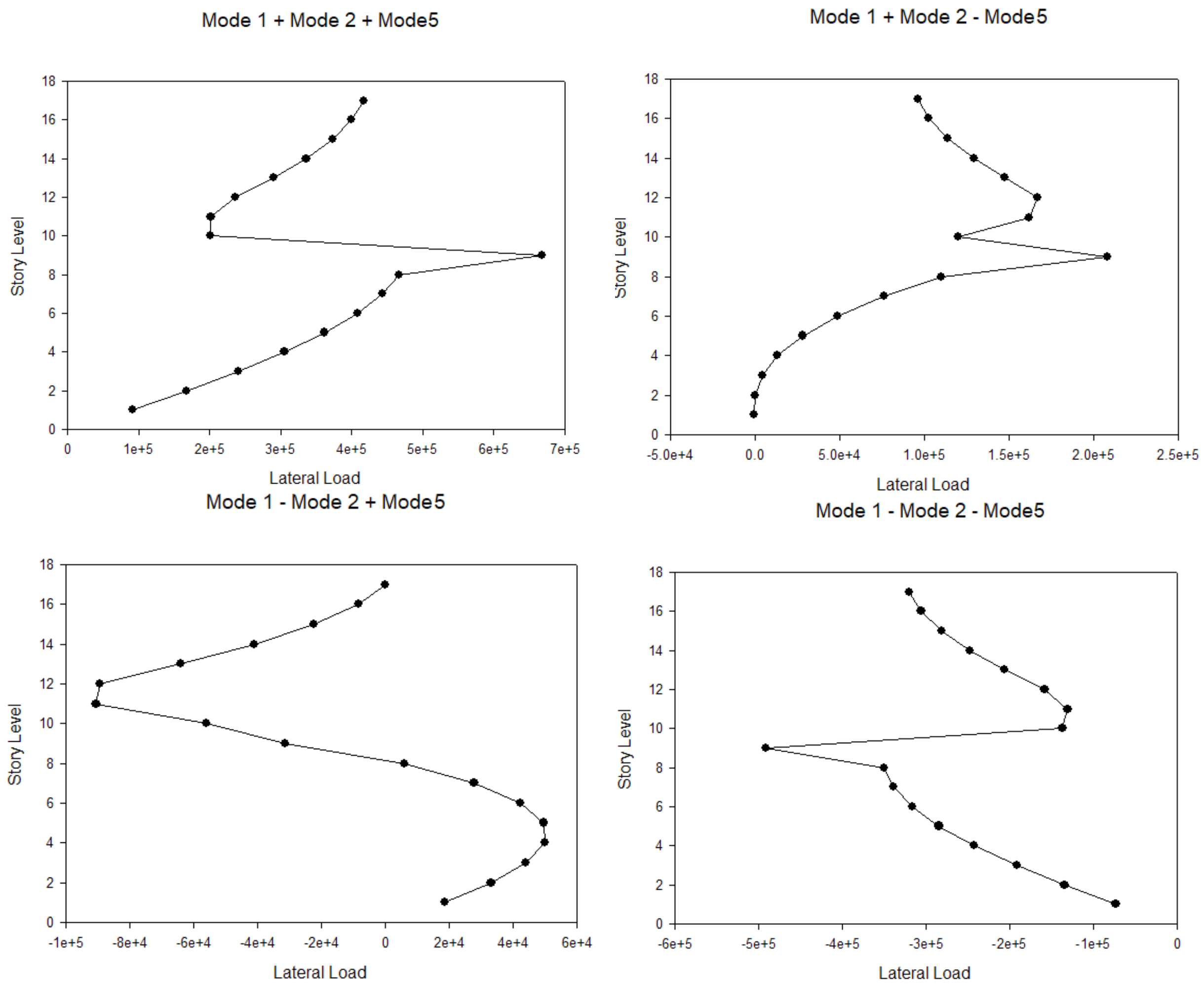


Fig 12

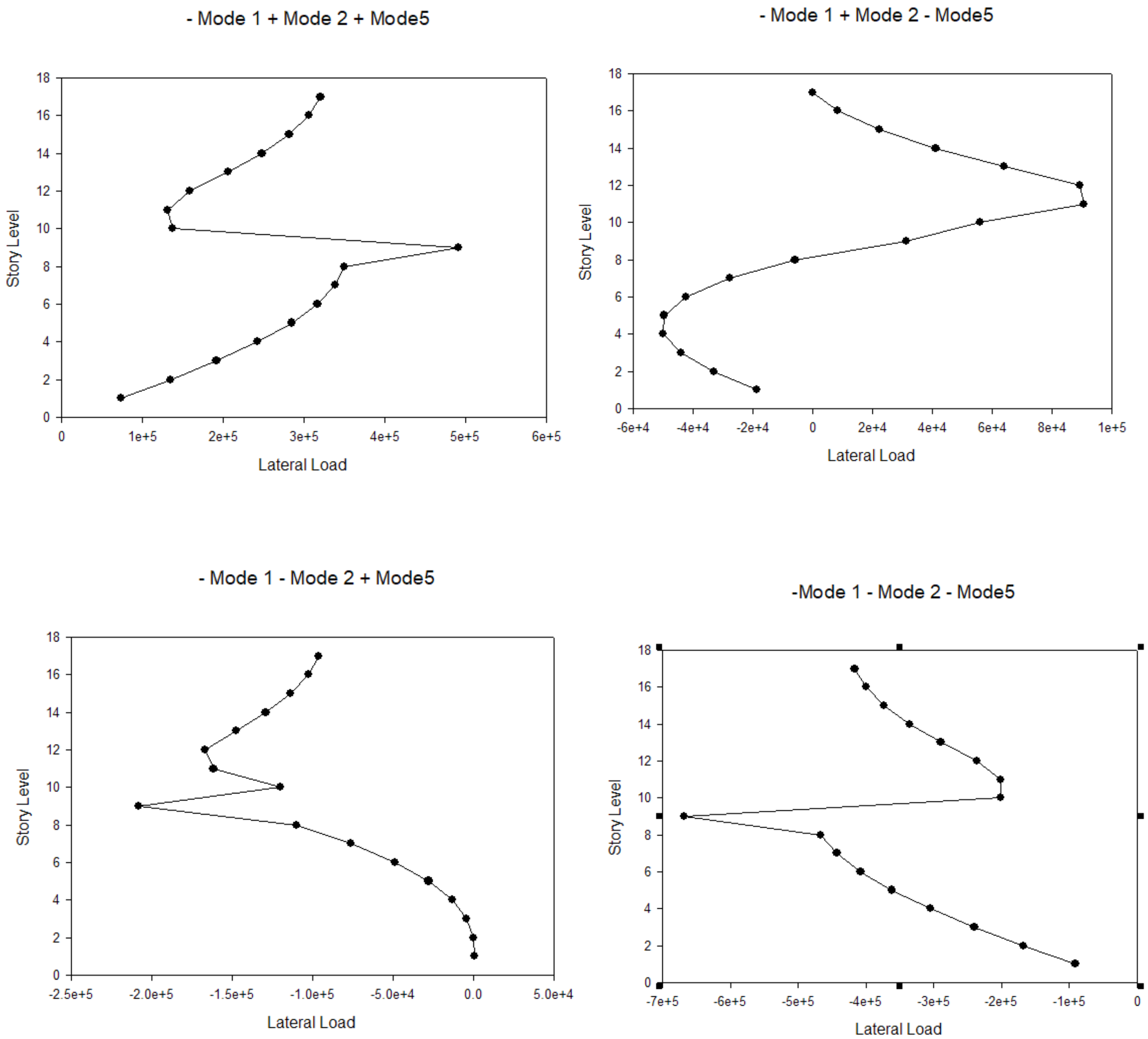
- Mode 1 + Mode 2 + Mode5
Story Level
Lateral Load
0
1e+5
2e+5
3e+5
4e+5
5e+5
6e+5
- Mode 1 + Mode 2 - Mode5
Story Level
Lateral Load
-6e+4
-4e+4
-2e+4
0
2e+4
4e+4
6e+4
8e+4
1e+5
- Mode 1 - Mode 2 + Mode5
Story Level
Lateral Load
-2.5e+5
-2.0e+5
-1.5e+5
-1.0e+5
-5.0e+4
0.0
5.0e+4
-Mode 1 - Mode 2 - Mode5
Story Level
Lateral Load
-7e+5
-6e+5
-5e+5
-4e+5
-3e+5
-2e+5
-1e+5
0

Fig 13

**Lateral Load Pattern for Y direction**

Based on the combination on the mode shapes of mode 1,2 and 4

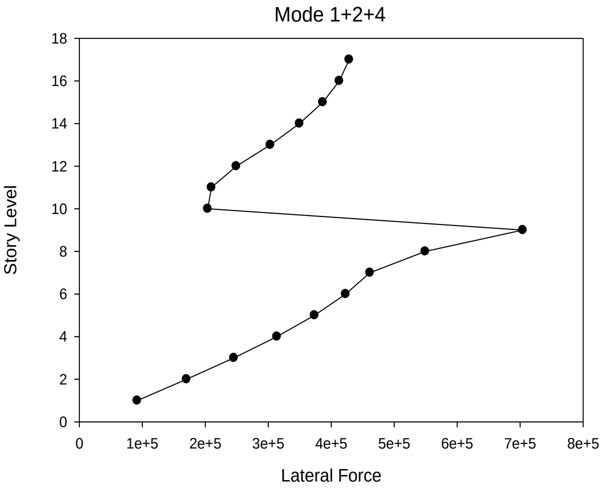


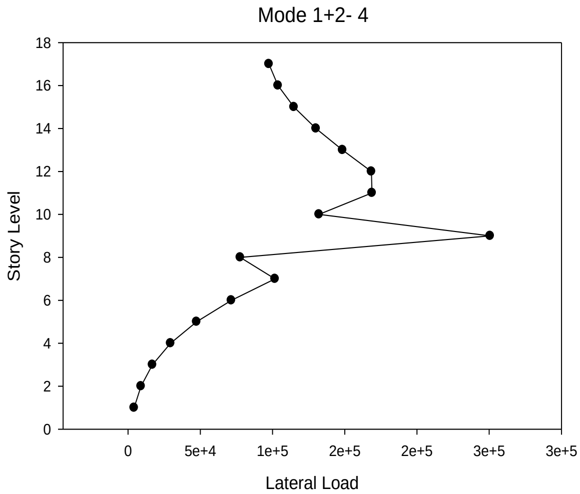


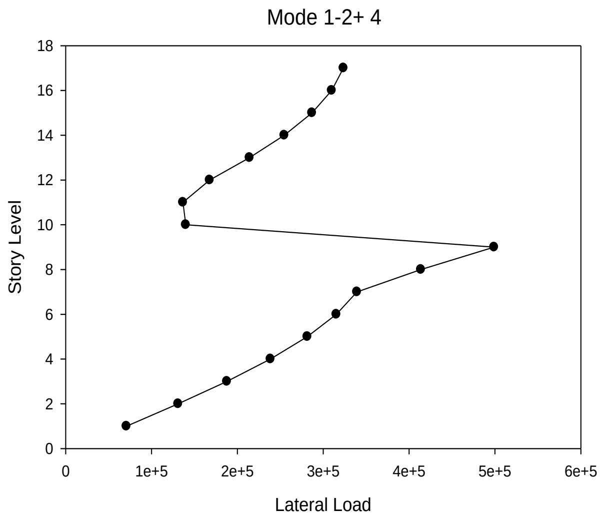


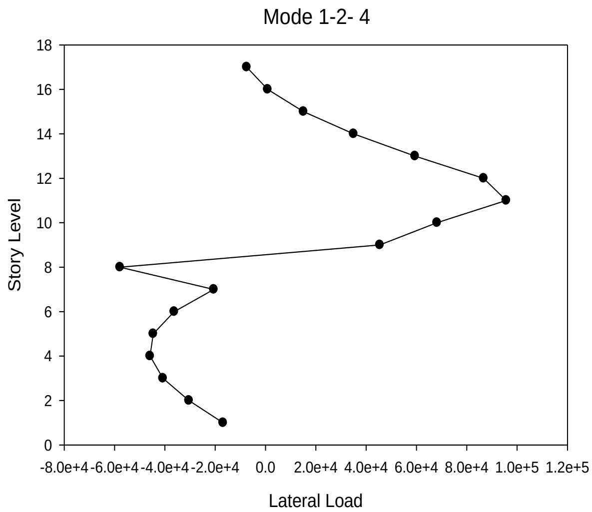


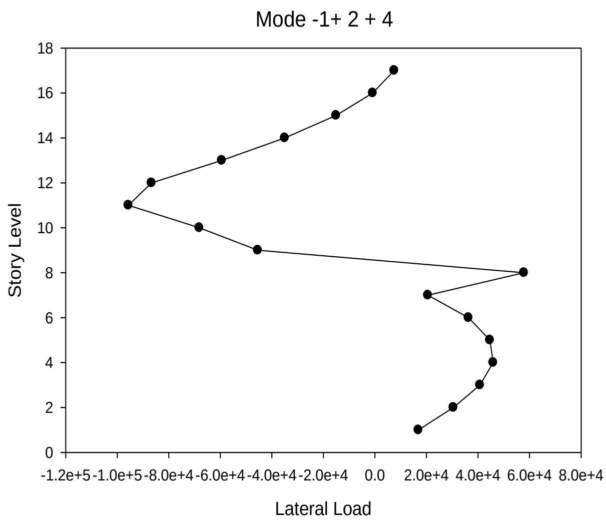


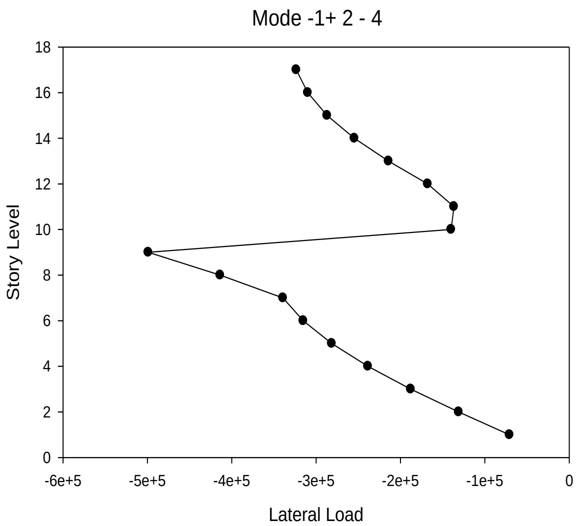

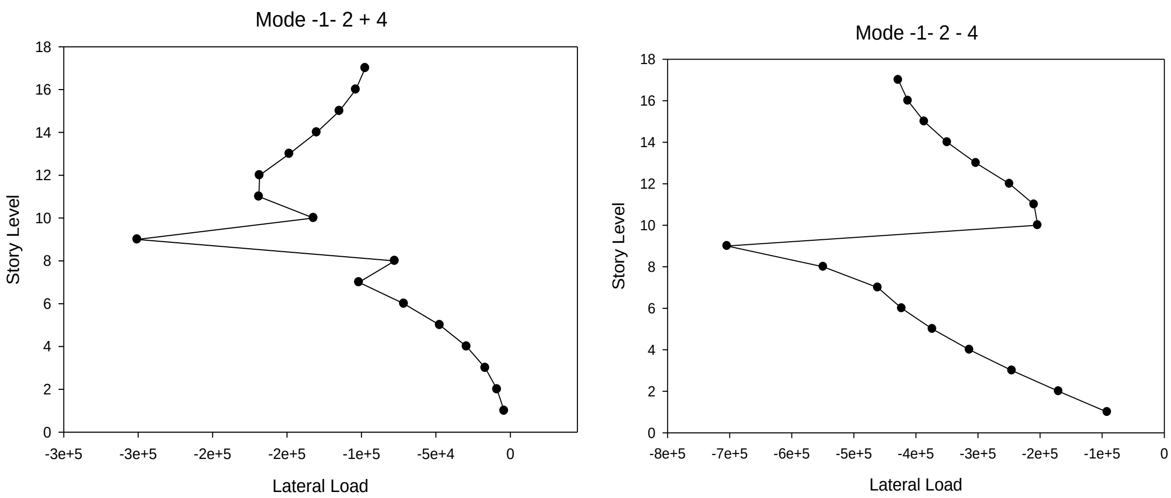
Mode -1- 2 + 4
Story Level
Lateral Load
0
2
4
6
8
10
12
14
16
18
-3e+5
-3e+5
-2e+5
-2e+5
-1e+5
-5e+4
0
Mode -1- 2 - 4
Story Level
Lateral Load
-8e+5
-7e+5
-6e+5
-5e+5
-4e+5
-3e+5
-2e+5
-1e+5
0

Fig 14

### 4.7 Pushover Analysis Result Comparison

Results of different types of pushover analysis are mentioned below. These results are compared with nonlinear time history analysis. The results which are in proximity of nonlinear time history analysis will be considered as most accurate.

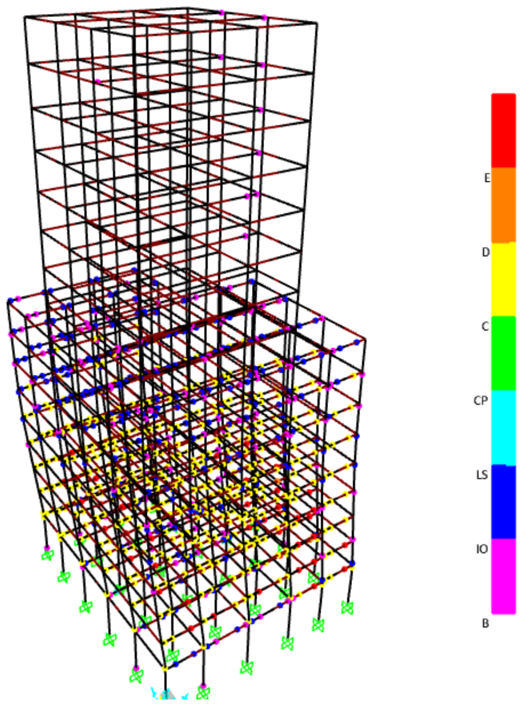


Fig 15
Conventional Pushover Analysis Pic

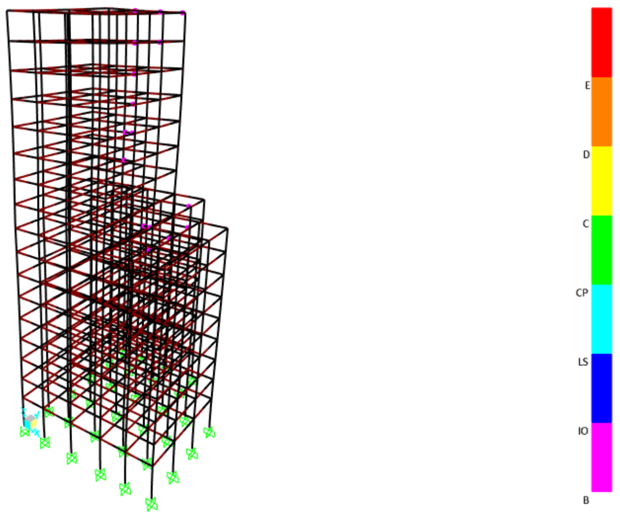


Fig 16
Modal Pushover Analysis

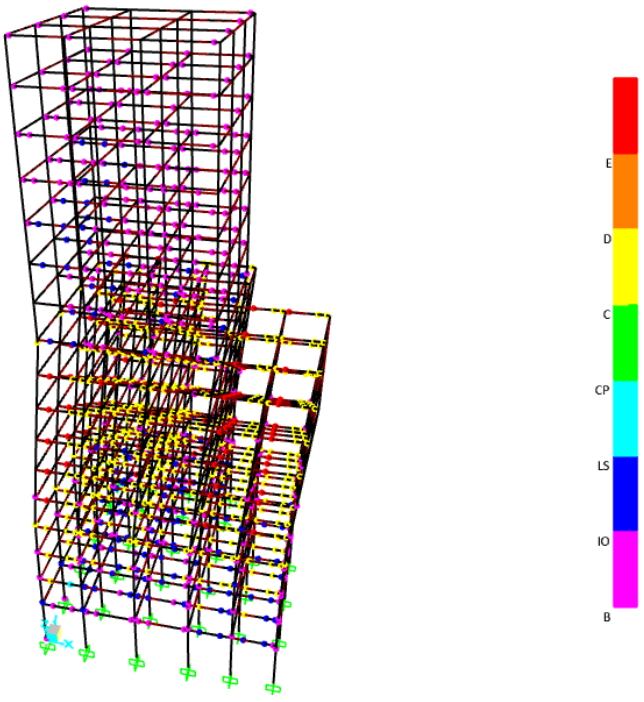


Fig 17
Modal Combination Analysis

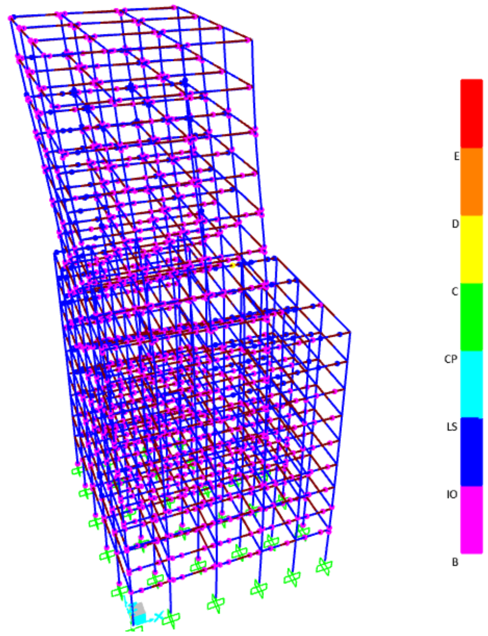


Fig 18
Nonlinear Time History (Elcentro)

From the results, it is clear that in case of the nonlinear time history analysis, the whole of the structure participates and from top to bottom plastic hinges are formed. While in the case of Pushover analysis, because the load isn’t reversing in nature only a particular shape of the load is applied because of which in case of typical pushover analysis case lower part of the structure yields. While in the case of model pushover analysis, the load is applied to correspond to the shape of a particular mode, because of which only those levels yields which are critical for that mode.

Modal combination analysis is the most specialized form of Pushover analysis as in this caseload shape, which is derived from the combination of modes, is applied. Because of this, the assigned lateral load carries a shape which is critical to all the stories. Hence the results of the Modal Pushover analysis are most accurate in comparison to other forms of Pushover analysis.

Nonlinear time history analysis gives the most accurate results. So, to predict the actual behavior of the structure Nonlinear time history analysis is the best solution. But, there aren’t enough time histories available. It can be just impossible to find a time history nearby of a particular site. Hence, modal combination pushover analysis is the best alternative to the Nonlinear time history analysis.

# CHAPTER 5

# RESULTS

Results for Modal Combination Pushover analysis in the X direction

**Modal Combination Mode(1+2+5) at 1% Drift**

| | BEAMS (Hinge Status) | | | COLUMNS (Hinge Status) | | |
|---|---|---|---|---|---|---|
| Floor Level | B-IO | IO-LS | LS-CP | B-IO | IO-LS | LS-CP |
| 1 | 35 | 0 | 0 | 0 | 0 | 0 |
| 2 | 50 | 0 | 0 | 0 | 0 | 0 |
| 3 | 52 | 0 | 0 | 0 | 0 | 0 |
| 4 | 52 | 0 | 0 | 0 | 0 | 0 |
| 5 | 51 | 0 | 0 | 0 | 0 | 0 |
| 6 | 37 | 0 | 0 | 0 | 0 | 0 |
| 7 | 32 | 0 | 0 | 0 | 0 | 0 |
| 8 | 31 | 0 | 0 | 0 | 0 | 0 |
| 9 | 29 | 0 | 0 | 0 | 0 | 0 |
| 10 | 7 | 0 | 0 | 0 | 0 | 0 |
| 11 | 6 | 0 | 0 | 0 | 0 | 0 |
| 12 | 6 | 0 | 0 | 0 | 0 | 0 |
| 13 | 5 | 0 | 0 | 0 | 0 | 0 |
| 14 | 4 | 0 | 0 | 0 | 0 | 0 |
| 15 | 5 | 0 | 0 | 0 | 0 | 0 |
| 16 | 6 | 0 | 0 | 0 | 0 | 0 |
| 17 | 4 | 0 | 0 | 0 | 0 | 0 |

Table 14

**Modal Combination Mode(-1+2+5) at 1% Drift**

| | BEAMS (Hinge Status) | | | COLUMNS (Hinge Status) | | |
|---|---|---|---|---|---|---|
| Floor Level | B-IO | IO-LS | LS-CP | B-IO | IO-LS | LS-CP |
| 1 | 52 | 0 | 0 | 1 P-M-M | 0 | 0 |
| 2 | 52 | 0 | 0 | 0 | 0 | 0 |
| 3 | 52 | 0 | 0 | 0 | 0 | 0 |
| 4 | 49 | 3 | 0 | 0 | 0 | 0 |
| 5 | 49 | 3 | 0 | 0 | 0 | 0 |
| 6 | 50 | 2 | 0 | 0 | 0 | 0 |
| 7 | 52 | 0 | 0 | 0 | 0 | 0 |
| 8 | 52 | 0 | 0 | 0 | 0 | 0 |
| 9 | 52 | 0 | 0 | 0 | 0 | 0 |
| 10 | 12 | 0 | 0 | 0 | 0 | 0 |
| 11 | 11 | 0 | 0 | 0 | 0 | 0 |
| 12 | 11 | 0 | 0 | 0 | 0 | 0 |
| 13 | 11 | 0 | 0 | 0 | 0 | 0 |
| 14 | 11 | 0 | 0 | 0 | 0 | 0 |
| 15 | 11 | 0 | 0 | 0 | 0 | 0 |
| 16 | 13 | 0 | 0 | 0 | 0 | 0 |
| 17 | 8 | 0 | 0 | 0 | 0 | 0 |

Table 15

**Modal Combination Mode(1+2-5) at 1% Drift**

| | BEAMS (Hinge Status) | | | COLUMNS (Hinge Status) | | |
|---|---|---|---|---|---|---|
| Floor Level | B-IO | IO-LS | LS-CP | B-IO | IO-LS | LS-CP |
| 1 | 32 | 0 | 0 | 1 P-M-M | 0 | 0 |
| 2 | 52 | 0 | 0 | 0 | 0 | 0 |
| 3 | 52 | 0 | 0 | 0 | 0 | 0 |
| 4 | 41 | 11 | 0 | 0 | 0 | 0 |
| 5 | 35 | 17 | 0 | 0 | 0 | 0 |
| 6 | 36 | 16 | 0 | 0 | 0 | 0 |
| 7 | 42 | 10 | 0 | 0 | 0 | 0 |
| 8 | 44 | 8 | 0 | 0 | 0 | 0 |
| 9 | 44 | 8 | 0 | 0 | 0 | 0 |
| 10 | 0 | 24 | 0 | 0 | 0 | 0 |
| 11 | 0 | 24 | 0 | 0 | 0 | 0 |
| 12 | 24 | 0 | 0 | 0 | 0 | 0 |
| 13 | 18 | 0 | 0 | 0 | 0 | 0 |
| 14 | 3 | 0 | 0 | 0 | 0 | 0 |
| 15 | 0 | 0 | 0 | 0 | 0 | 0 |
| 16 | 0 | 0 | 0 | 0 | 0 | 0 |
| 17 | 0 | 0 | 0 | 0 | 0 | 0 |

Table 16

**Modal Combination Mode(-1+2-5) at 1% Drift**

| | BEAMS (Hinge Status) | | | COLUMNS (Hinge Status) | | |
|---|---|---|---|---|---|---|
| Floor Level | B-IO | IO-LS | LS-CP | B-IO | IO-LS | LS-CP |
| 1 | 0 | 0 | 0 | 1 P-M-M | 0 | 0 |
| 2 | 0 | 0 | 0 | 0 | 0 | 0 |
| 3 | 0 | 0 | 0 | 0 | 0 | 0 |
| 4 | 11 | 0 | 0 | 0 | 0 | 0 |
| 5 | 31 | 0 | 0 | 0 | 0 | 0 |
| 6 | 48 | 0 | 0 | 0 | 0 | 0 |
| 7 | 52 | 0 | 0 | 0 | 0 | 0 |
| 8 | 37 | 15 | 0 | 0 | 0 | 0 |
| 9 | 38 | 14 | 0 | 0 | 0 | 0 |
| 10 | 0 | 0 | 24 | 0 | 0 | 0 |
| 11 | 0 | 0 | 24 | 0 | 0 | 0 |
| 12 | 0 | 24 | 0 | 0 | 0 | 0 |
| 13 | 24 | 0 | 0 | 0 | 0 | 0 |
| 14 | 3 | 0 | 0 | 0 | 0 | 0 |
| 15 | 0 | 0 | 0 | 0 | 0 | 0 |
| 16 | 0 | 0 | 0 | 0 | 0 | 0 |
| 17 | 0 | 0 | 0 | 0 | 0 | 0 |

Table 17

**Modal Combination Mode(-1-2+5) at 1% Drift**

| | BEAMS (Hinge Status) | | | COLUMNS (Hinge Status) | | |
|---|---|---|---|---|---|---|
| Floor Level | B-IO | IO-LS | LS-CP | B-IO | IO-LS | LS-CP |
| 1 | 35 | 0 | 0 | 0 | 0 | 0 |
| 2 | 52 | 0 | 0 | 0 | 0 | 0 |
| 3 | 52 | 0 | 0 | 0 | 0 | 0 |
| 4 | 40 | 12 | 0 | 0 | 0 | 0 |
| 5 | 35 | 17 | 0 | 0 | 0 | 0 |
| 6 | 36 | 16 | 0 | 0 | 0 | 0 |
| 7 | 40 | 12 | 0 | 0 | 0 | 0 |
| 8 | 47 | 5 | 0 | 0 | 0 | 0 |
| 9 | 44 | 8 | 0 | 0 | 0 | 0 |
| 10 | 0 | 24 | 0 | 0 | 0 | 0 |
| 11 | 2 | 22 | 0 | 0 | 0 | 0 |
| 12 | 24 | 0 | 0 | 0 | 0 | 0 |
| 13 | 16 | 0 | 0 | 0 | 0 | 0 |
| 14 | 2 | 0 | 0 | 0 | 0 | 0 |
| 15 | 0 | 0 | 0 | 0 | 0 | 0 |
| 16 | 0 | 0 | 0 | 0 | 0 | 0 |
| 17 | 0 | 0 | 0 | 0 | 0 | 0 |

Table 18

**Modal Combination Mode(1-2+5) at 1% Drift**

| | BEAMS (Hinge Status) | | | COLUMNS (Hinge Status) | | |
|---|---|---|---|---|---|---|
| Floor Level | B-IO | IO-LS | LS-CP | B-IO | IO-LS | LS-CP |
| 1 | 0 | 0 | 0 | 0 | 0 | 0 |
| 2 | 0 | 0 | 0 | 0 | 0 | 0 |
| 3 | 0 | 0 | 0 | 0 | 0 | 0 |
| 4 | 0 | 12 | 0 | 0 | 0 | 0 |
| 5 | 20 | 17 | 0 | 0 | 0 | 0 |
| 6 | 52 | 0 | 0 | 0 | 0 | 0 |
| 7 | 41 | 11 | 0 | 0 | 0 | 0 |
| 8 | 0 | 52 | 0 | 0 | 0 | 0 |
| 9 | 1(y) | 52 | 0 | 0 | 0 | 0 |
| 10 | 0 | 24 | 0 | 0 | 0 | 0 |
| 11 | 2 | 22 | 0 | 0 | 0 | 0 |
| 12 | 24 | 0 | 0 | 0 | 0 | 0 |
| 13 | 1 | 0 | 0 | 0 | 0 | 0 |
| 14 | 0 | 0 | 0 | 0 | 0 | 0 |
| 15 | 0 | 0 | 0 | 0 | 0 | 0 |
| 16 | 0 | 0 | 0 | 0 | 0 | 0 |
| 17 | 0 | 0 | 0 | 0 | 0 | 0 |

Table 19

**Modal Combination Mode(1-2-5) at 1% Drift**

| | BEAMS (Hinge Status) | | | COLUMNS (Hinge Status) | | |
|---|---|---|---|---|---|---|
| Floor Level | B-IO | IO-LS | LS-CP | B-IO | IO-LS | LS-CP |
| 1 | 52 | 0 | 0 | 0 | 0 | 0 |
| 2 | 52 | 0 | 0 | 0 | 0 | 0 |
| 3 | 51 | 1 | 0 | 0 | 0 | 0 |
| 4 | 48 | 4 | 0 | 0 | 0 | 0 |
| 5 | 48 | 4 | 0 | 0 | 0 | 0 |
| 6 | 50 | 2 | 0 | 0 | 0 | 0 |
| 7 | 52 | 0 | 0 | 0 | 0 | 0 |
| 8 | 52 | 0 | 0 | 0 | 0 | 0 |
| 9 | 52 | 0 | 0 | 0 | 0 | 0 |
| 10 | 19 | 0 | 0 | 0 | 0 | 0 |
| 11 | 10 | 0 | 0 | 0 | 0 | 0 |
| 12 | 8 | 0 | 0 | 0 | 0 | 0 |
| 13 | 8 | 0 | 0 | 0 | 0 | 0 |
| 14 | 7 | 0 | 0 | 0 | 0 | 0 |
| 15 | 7 | 0 | 0 | 0 | 0 | 0 |
| 16 | 8 | 0 | 0 | 0 | 0 | 0 |
| 17 | 3 | 0 | 0 | 0 | 0 | 0 |

Table 20

**Modal Combination Mode(-1-2-5) at 1% Drift**

| | BEAMS (Hinge Status) | | | COLUMNS (Hinge Status) | | |
|---|---|---|---|---|---|---|
| Floor Level | B-IO | IO-LS | LS-CP | B-IO | IO-LS | LS-CP |
| 1 | 52 | 0 | 0 | 0 | 0 | 0 |
| 2 | 52 | 0 | 0 | 0 | 0 | 0 |
| 3 | 48 | 4 | 0 | 0 | 0 | 0 |
| 4 | 42 | 10 | 0 | 0 | 0 | 0 |
| 5 | 45 | 7 | 0 | 0 | 0 | 0 |
| 6 | 50 | 2 | 0 | 0 | 0 | 0 |
| 7 | 52 | 0 | 0 | 0 | 0 | 0 |
| 8 | 52 | 0 | 0 | 0 | 0 | 0 |
| 9 | 52 | 0 | 0 | 0 | 0 | 0 |
| 10 | 8 | 0 | 0 | 0 | 0 | 0 |
| 11 | 4 | 0 | 0 | 0 | 0 | 0 |
| 12 | 3 | 0 | 0 | 0 | 0 | 0 |
| 13 | 2 | 0 | 0 | 0 | 0 | 0 |
| 14 | 2 | 0 | 0 | 0 | 0 | 0 |
| 15 | 2 | 0 | 0 | 0 | 0 | 0 |
| 16 | 4 | 0 | 0 | 0 | 0 | 0 |
| 17 | 2 | 0 | 0 | 0 | 0 | 0 |

Table 21

**Results for Modal Combination Pushover analysis in Y direction**

**Modal Combination Mode(1+2+4) at 1% Drift**

| | BEAMS (Hinge Status) | | | COLUMNS (Hinge Status) | | |
|---|---|---|---|---|---|---|
| Floor Level | B-IO | IO-LS | LS-CP | B-IO | IO-LS | LS-CP |
| 1 | 52 | 0 | 0 | 0 | 0 | 0 |
| 2 | 45 | 7 | 0 | 0 | 0 | 0 |
| 3 | 12 | 40 | 0 | 0 | 0 | 0 |
| 4 | 52 | 0 | 0 | 0 | 0 | 0 |
| 5 | 52 | 0 | 0 | 0 | 0 | 0 |
| 6 | 8 | 44 | 0 | 0 | 0 | 0 |
| 7 | 35 | 17 | 0 | 0 | 0 | 0 |
| 8 | 50 | 2 | 0 | 0 | 0 | 0 |
| 9 | 52 | 0 | 0 | 0 | 0 | 0 |
| 10 | 11 | 0 | 0 | 0 | 0 | 0 |
| 11 | 3 | 0 | 0 | 0 | 0 | 0 |
| 12 | 3 | 0 | 0 | 0 | 0 | 0 |
| 13 | 3 | 0 | 0 | 0 | 0 | 0 |
| 14 | 3 | 0 | 0 | 0 | 0 | 0 |
| 15 | 3 | 0 | 0 | 0 | 0 | 0 |
| 16 | 3 | 0 | 0 | 0 | 0 | 0 |
| 17 | 0 | 0 | 0 | 0 | 0 | 0 |

Table 22

**Modal Combination Mode(-1+2+4) at 1% Drift**

| | BEAMS (Hinge Status) | | | COLUMNS (Hinge Status) | | |
|---|---|---|---|---|---|---|
| Floor Level | B-IO | IO-LS | LS-CP | B-IO | IO-LS | LS-CP |
| 1 | 0 | 0 | 0 | 0 | 0 | 0 |
| 2 | 0 | 0 | 0 | 0 | 0 | 0 |
| 3 | 0 | 0 | 0 | 0 | 0 | 0 |
| 4 | 2 | 0 | 0 | 0 | 0 | 0 |
| 5 | 37 | 0 | 0 | 0 | 0 | 0 |
| 6 | 52 | 0 | 0 | 0 | 0 | 0 |
| 7 | 23 | 29 | 0 | 0 | 0 | 0 |
| 8 | 52 | 0 | 0 | 0 | 0 | 0 |
| 9 | 52 | 0 | 0 | 0 | 0 | 0 |
| 10 | 23 | 0 | 1 | 0 | 0 | 0 |
| 11 | 22 | 2 | 0 | 0 | 0 | 0 |
| 12 | 23 | 0 | 0 | 0 | 0 | 0 |
| 13 | 2 | 0 | 0 | 0 | 0 | 0 |
| 14 | 0 | 0 | 0 | 0 | 0 | 0 |
| 15 | 0 | 0 | 0 | 0 | 0 | 0 |
| 16 | 0 | 0 | 0 | 0 | 0 | 0 |
| 17 | 0 | 0 | 0 | 0 | 0 | 0 |

Table 23

**Modal Combination Mode(-1+2-4) at 1% Drift**

| | BEAMS (Hinge Status) | | | COLUMNS (Hinge Status) | | |
|---|---|---|---|---|---|---|
| Floor Level | B-IO | IO-LS | LS-CP | B-IO | IO-LS | LS-CP |
| 1 | 52 | 0 | 0 | 0 | 0 | 0 |
| 2 | 50 | 2 | 0 | 0 | 0 | 0 |
| 3 | 27 | 25 | 0 | 0 | 0 | 0 |
| 4 | 10 | 42 | 0 | 0 | 0 | 0 |
| 5 | 10 | 42 | 0 | 0 | 0 | 0 |
| 6 | 27 | 25 | 0 | 0 | 0 | 0 |
| 7 | 43 | 9 | 0 | 0 | 0 | 0 |
| 8 | 51 | 1 | 0 | 0 | 0 | 0 |
| 9 | 52 | 0 | 0 | 0 | 0 | 0 |
| 10 | 12 | 0 | 0 | 0 | 0 | 0 |
| 11 | 2 | 0 | 0 | 0 | 0 | 0 |
| 12 | 2 | 0 | 0 | 0 | 0 | 0 |
| 13 | 2 | 0 | 0 | 0 | 0 | 0 |
| 14 | 2 | 0 | 0 | 0 | 0 | 0 |
| 15 | 2 | 0 | 0 | 0 | 0 | 0 |
| 16 | 2 | 0 | 0 | 0 | 0 | 0 |
| 17 | 2 | 0 | 0 | 0 | 0 | 0 |

Table 24

**Modal Combination Mode(1-2+4) at 1% Drift**

| | BEAMS (Hinge Status) | | | COLUMNS (Hinge Status) | | |
|---|---|---|---|---|---|---|
| Floor Level | B-IO | IO-LS | LS-CP | B-IO | IO-LS | LS-CP |
| 1 | 50 | 0 | 0 | 0 | 0 | 0 |
| 2 | 51 | 1 | 0 | 0 | 0 | 0 |
| 3 | 29 | 23 | 0 | 0 | 0 | 0 |
| 4 | 11 | 41 | 0 | 0 | 0 | 0 |
| 5 | 12 | 40 | 0 | 0 | 0 | 0 |
| 6 | 12 | 40 | 0 | 0 | 0 | 0 |
| 7 | 26 | 26 | 0 | 0 | 0 | 0 |
| 8 | 44 | 8 | 0 | 0 | 0 | 0 |
| 9 | 52 | 0 | 0 | 0 | 0 | 0 |
| 10 | 52 | 0 | 0 | 0 | 0 | 0 |
| 11 | 11 | 0 | 0 | 0 | 0 | 0 |
| 12 | 4 | 0 | 0 | 0 | 0 | 0 |
| 13 | 3 | 0 | 0 | 0 | 0 | 0 |
| 14 | 3 | 0 | 0 | 0 | 0 | 0 |
| 15 | 3 | 0 | 0 | 0 | 0 | 0 |
| 16 | 3 | 0 | 0 | 0 | 0 | 0 |
| 17 | 3 | 0 | 0 | 0 | 0 | 0 |

Table 25

**Modal Combination Mode(1+2-4) at 1% Drift**

| | BEAMS (Hinge Status) | | | COLUMNS (Hinge Status) | | |
|---|---|---|---|---|---|---|
| Floor Level | B-IO | IO-LS | LS-CP | B-IO | IO-LS | LS-CP |
| 1 | 13 | 0 | 0 | 0 | 0 | 0 |
| 2 | 38 | 0 | 0 | 0 | 0 | 0 |
| 3 | 52 | 0 | 0 | 0 | 0 | 0 |
| 4 | 52 | 0 | 0 | 0 | 0 | 0 |
| 5 | 43 | 9 | 0 | 0 | 0 | 0 |
| 6 | 27 | 25 | 0 | 0 | 0 | 0 |
| 7 | 8 | 44 | 0 | 0 | 0 | 0 |
| 8 | 1 | 51 | 0 | 0 | 0 | 0 |
| 9 | 47 | 5 | 0 | 0 | 0 | 0 |
| 10 | 23 | 1 | 0 | 0 | 0 | 0 |
| 11 | 17 | 0 | 0 | 0 | 0 | 0 |
| 12 | 7 | 0 | 0 | 0 | 0 | 0 |
| 13 | 2 | 0 | 0 | 0 | 0 | 0 |
| 14 | 0 | 0 | 0 | 0 | 0 | 0 |
| 15 | 0 | 0 | 0 | 0 | 0 | 0 |
| 16 | 1 | 0 | 0 | 0 | 0 | 0 |
| 17 | 1 | 0 | 0 | 0 | 0 | 0 |

Table 26

**Modal Combination Mode(-1-2+4) at 1% Drift**

| | BEAMS (Hinge Status) | | | COLUMNS (Hinge Status) | | |
|---|---|---|---|---|---|---|
| Floor Level | B-IO | IO-LS | LS-CP | B-IO | IO-LS | LS-CP |
| 1 | 18 | 0 | 0 | 0 | 0 | 0 |
| 2 | 38 | 0 | 0 | 0 | 0 | 0 |
| 3 | 52 | 0 | 0 | 0 | 0 | 0 |
| 4 | 52 | 0 | 0 | 0 | 0 | 0 |
| 5 | 39 | 13 | 0 | 0 | 0 | 0 |
| 6 | 26 | 26 | 0 | 0 | 0 | 0 |
| 7 | 9 | 43 | 0 | 0 | 0 | 0 |
| 8 | 4 | 48 | 0 | 0 | 0 | 0 |
| 9 | 6 | 46 | 0 | 0 | 0 | 0 |
| 10 | 23 | 1 | 0 | 0 | 0 | 0 |
| 11 | 19 | 0 | 0 | 0 | 0 | 0 |
| 12 | 5 | 0 | 0 | 0 | 0 | 0 |
| 13 | 2 | 0 | 0 | 0 | 0 | 0 |
| 14 | 1 | 0 | 0 | 0 | 0 | 0 |
| 15 | 1 | 0 | 0 | 0 | 0 | 0 |
| 16 | 1 | 0 | 0 | 0 | 0 | 0 |
| 17 | 2 | 0 | 0 | 0 | 0 | 0 |

Table 27

**Modal Combination Mode(1-2-4) at 1% Drift**

| | BEAMS (Hinge Status) | | | COLUMNS (Hinge Status) | | |
|---|---|---|---|---|---|---|
| Floor Level | B-IO | IO-LS | LS-CP | B-IO | IO-LS | LS-CP |
| 1 | 0 | 0 | 0 | 0 | 0 | 0 |
| 2 | 0 | 0 | 0 | 0 | 0 | 0 |
| 3 | 0 | 0 | 0 | 0 | 0 | 0 |
| 4 | 1 | 0 | 0 | 0 | 0 | 0 |
| 5 | 37 | 0 | 0 | 0 | 0 | 0 |
| 6 | 52 | 0 | 0 | 0 | 0 | 0 |
| 7 | 24 | 28 | 0 | 0 | 0 | 0 |
| 8 | 0 | 52 | 0 | 0 | 0 | 0 |
| 9 | 0 | 52 | 0 | 0 | 0 | 0 |
| 10 | 0 | 24 | 0 | 0 | 0 | 0 |
| 11 | 20 | 22 | 0 | 0 | 0 | 0 |
| 12 | 24 | 0 | 0 | 0 | 0 | 0 |
| 13 | 2 | 0 | 0 | 0 | 0 | 0 |
| 14 | 0 | 0 | 0 | 0 | 0 | 0 |
| 15 | 0 | 0 | 0 | 0 | 0 | 0 |
| 16 | 0 | 0 | 0 | 0 | 0 | 0 |
| 17 | 0 | 0 | 0 | 0 | 0 | 0 |

Table 28

**Modal Combination Mode(-1-2-4) at 1% Drift**

| | BEAMS (Hinge Status) | | | COLUMNS (Hinge Status) | | |
|---|---|---|---|---|---|---|
| Floor Level | B-IO | IO-LS | LS-CP | B-IO | IO-LS | LS-CP |
| 1 | 52 | 0 | 0 | 0 | 0 | 0 |
| 2 | 51 | 1 | 0 | 0 | 0 | 0 |
| 3 | 29 | 23 | 0 | 0 | 0 | 0 |
| 4 | 11 | 41 | 0 | 0 | 0 | 0 |
| 5 | 11 | 49 | 0 | 0 | 0 | 0 |
| 6 | 26 | 26 | 0 | 0 | 0 | 0 |
| 7 | 39 | 13 | 0 | 0 | 0 | 0 |
| 8 | 51 | 1 | 0 | 0 | 0 | 0 |
| 9 | 52 | 0 | 0 | 0 | 0 | 0 |
| 10 | 13 | 0 | 0 | 0 | 0 | 0 |
| 11 | 3 | 0 | 0 | 0 | 0 | 0 |
| 12 | 2 | 0 | 0 | 0 | 0 | 0 |
| 13 | 2 | 0 | 0 | 0 | 0 | 0 |
| 14 | 2 | 0 | 0 | 0 | 0 | 0 |
| 15 | 2 | 0 | 0 | 0 | 0 | 0 |
| 16 | 2 | 0 | 0 | 0 | 0 | 0 |
| 17 | 2 | 0 | 0 | 0 | 0 | 0 |

Table 29

## Non Linear Time History Analysis Results

**Elcentro**

Elcentro earthquake time history (fully scaled) was run on sap2000. It has a peak ground acceleration of $3.425 m/s^2$. Final state pictures are shown below depicting the damage sustained by the structure.

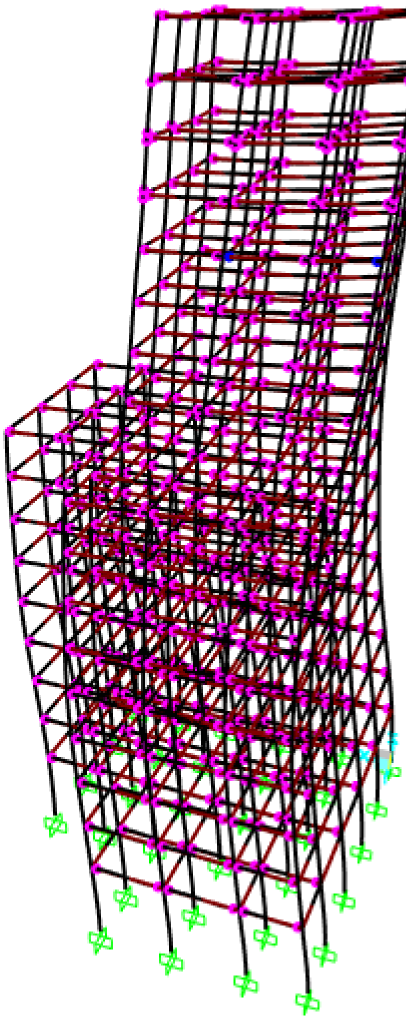

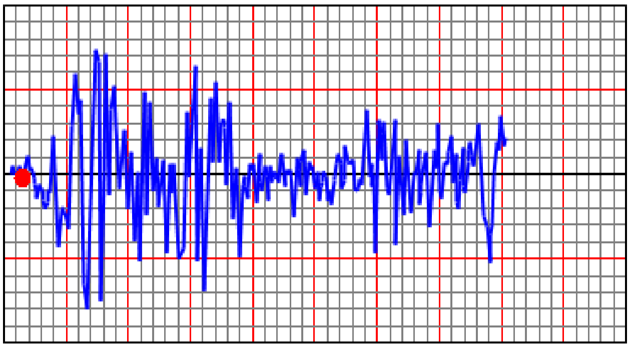

**Fig 19**

Following table shows the list of elements damaged severely and at the stage of Collapse prevention.

| Element ID | Number of Hinger >CP | Elemetn Type | Element ID | Number of Hinger >CP | Elemetn Type |
|---|---|---|---|---|---|
| 1131 | 1 | COLUMN | 1328 | 1 | COLUMN |
| 1132 | 1 | COLUMN | 1351 | 1 | COLUMN |
| 1133 | 2 | COLUMN | 1387 | 1 | COLUMN |
| 1134 | 1 | COLUMN | 1776 | 1 | COLUMN |
| 1135 | 2 | COLUMN | 1780 | 1 | COLUMN |
| 1136 | 2 | COLUMN | 1781 | 1 | COLUMN |
| 1137 | 2 | COLUMN | 1782 | 2 | COLUMN |
| 1138 | 1 | COLUMN | 1783 | 2 | COLUMN |
| 1146 | 1 | COLUMN | 1784 | 1 | COLUMN |
| 1179 | 1 | COLUMN | 1785 | 1 | COLUMN |
| 1185 | 1 | COLUMN | 1786 | 1 | COLUMN |
| 1186 | 1 | COLUMN | 1789 | 2 | COLUMN |
| 1187 | 2 | COLUMN | 1790 | 2 | COLUMN |
| 1188 | 1 | COLUMN | 1817 | 1 | COLUMN |
| 1189 | 1 | COLUMN | 1820 | 2 | COLUMN |
| 1190 | 2 | COLUMN | 1821 | 1 | COLUMN |
| 1191 | 2 | COLUMN | 1826 | 1 | COLUMN |
| 1192 | 1 | COLUMN | 1828 | 2 | COLUMN |
| 1196 | 1 | COLUMN | 1829 | 1 | COLUMN |
| 1205 | 2 | COLUMN | 1830 | 2 | COLUMN |
| 1228 | 1 | COLUMN | 1831 | 1 | COLUMN |
| 1240 | 1 | COLUMN | 1861 | 1 | COLUMN |
| 1241 | 1 | COLUMN | 1868 | 1 | COLUMN |
| 1242 | 2 | COLUMN | 1869 | 1 | COLUMN |
| 1243 | 2 | COLUMN | 1870 | 1 | COLUMN |
| 1244 | 2 | COLUMN | 1871 | 1 | COLUMN |
| 1245 | 2 | COLUMN | 1897 | 2 | COLUMN |
| 1246 | 2 | COLUMN | 1898 | 1 | COLUMN |
| 1274 | 1 | COLUMN | 1900 | 1 | COLUMN |
| 1303 | 1 | COLUMN | 1906 | 2 | COLUMN |
| 1304 | 1 | COLUMN | 1907 | 1 | COLUMN |
| 1305 | 2 | COLUMN | 1908 | 1 | COLUMN |
| 1306 | 2 | COLUMN | 1910 | 2 | COLUMN |
| 1308 | 1 | COLUMN | 1911 | 2 | COLUMN |
| 1310 | 1 | COLUMN | 1942 | 1 | COLUMN |
| 1327 | 1 | COLUMN | 1950 | 1 | COLUMN |
| 2026 | 1 | COLUMN | 1981 | 1 | COLUMN |
| 2030 | 1 | COLUMN | 1989 | 1 | COLUMN |
| 2070 | 1 | COLUMN | 1990 | 1 | COLUMN |

Table 30

**Chamoli**

Chamoli (1999) earthquake had a peak ground acceleration of 3.5 m/s$^2$. The ground motion used was recorded at Chamoli site.

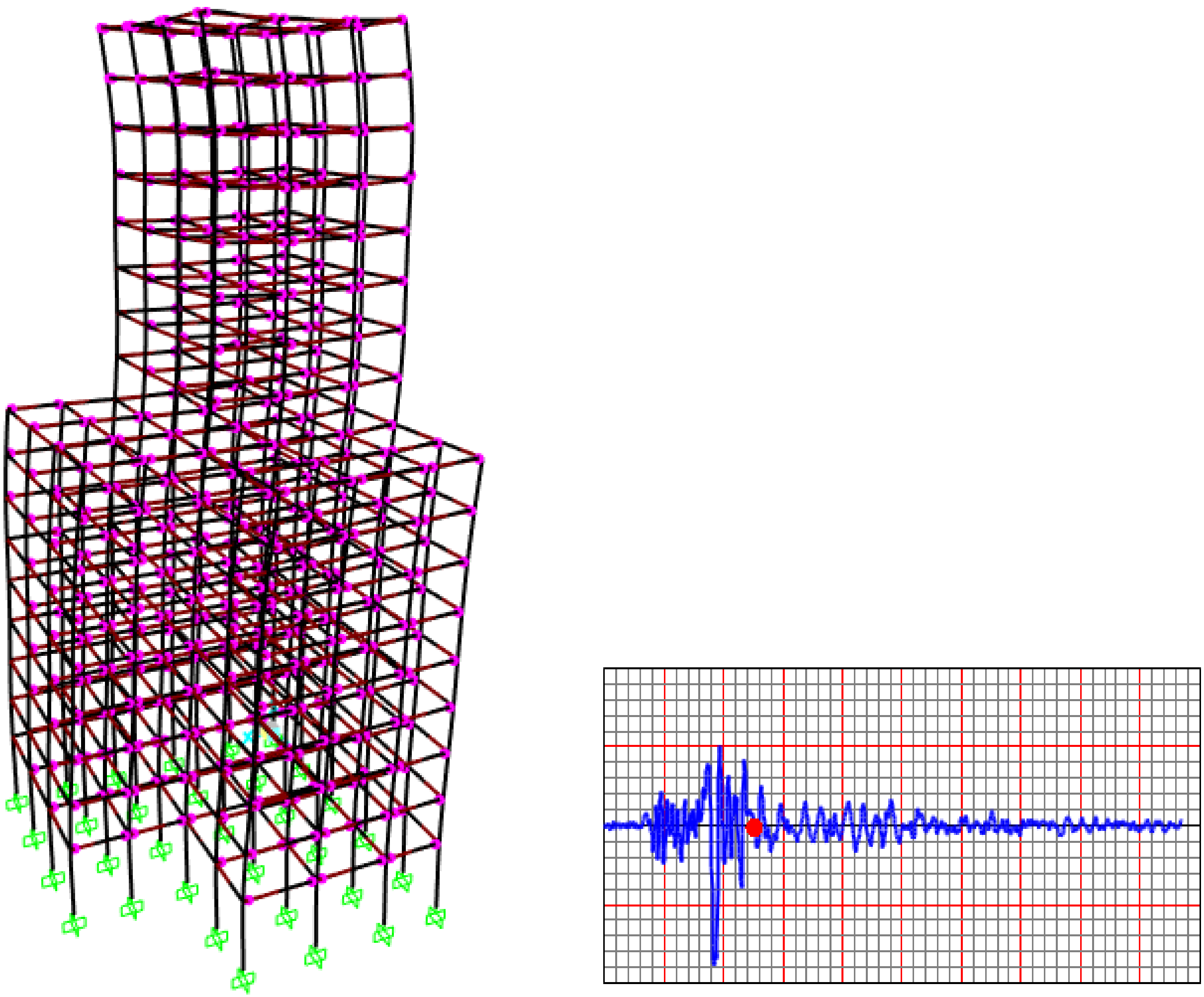

Fig 20

It's clear that all the hinges are in Immediate occupancy level of performance.

**Uttar Kashi**

Uttarkashi (1991) earthquake had a peak ground acceleration of 3.04 $m/s^2$. The ground motion used was recorded at Chamoli site.

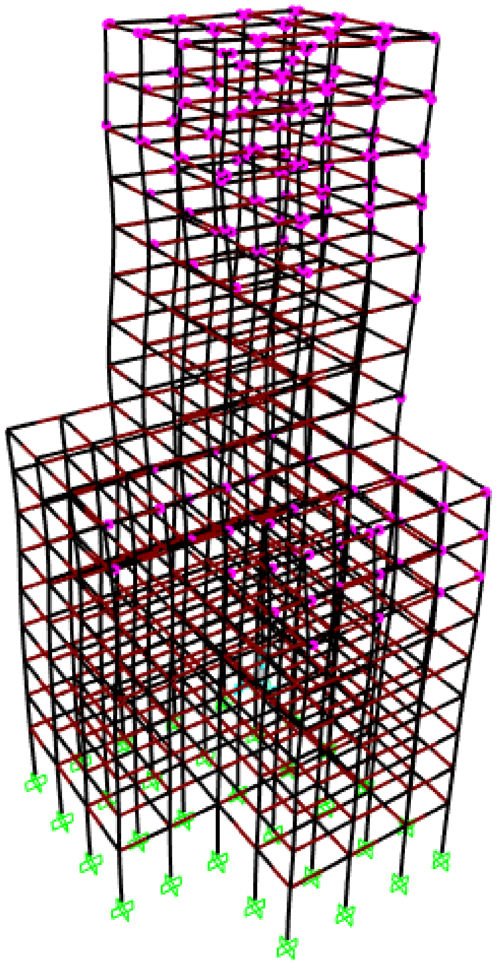

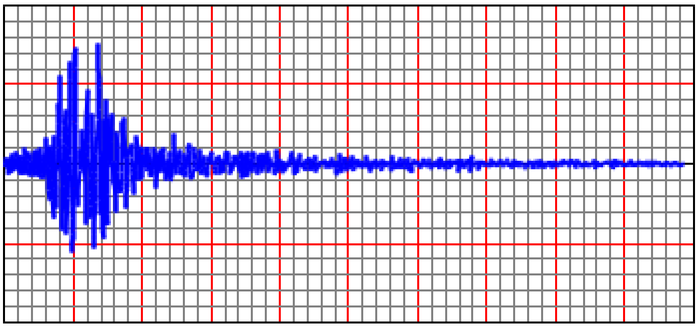

From the results of Modal Combination Analysis,and verified by NLTHA it is clear that the structure needs strengthening from Story Level four to eleven. Beams are mainly damaged, hence depth of the beams needs to be increased in such a way that strong Column Weak beam philosophy(Capacity Design) is strongly followed. The lateral deflection of the top is 240mm at the end of the earthquake.

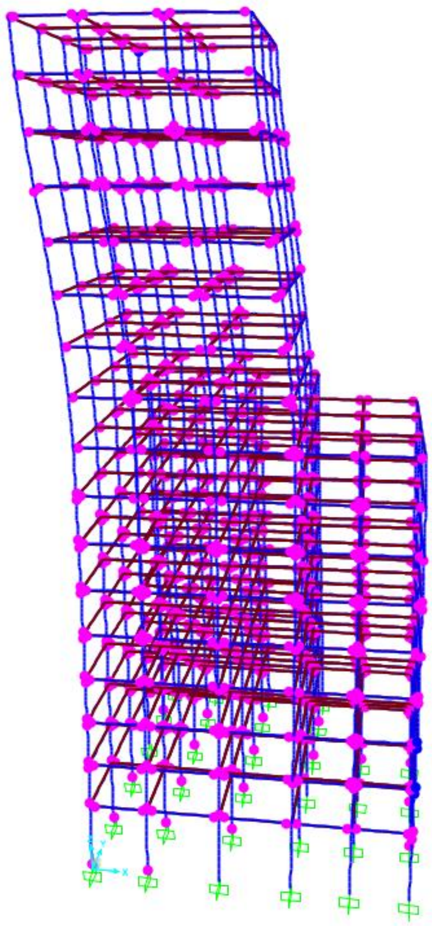

Fig 21

Results After Increasing beam stiffness (Elcentro)

| Frame ID | Number of Hinges(>CP) | Hinge Type |
|---|---|---|
| 1134 | 1 | P-M-M |
| 1165 | 1 | P-M-M |
| 1188 | 1 | P-M-M |
| 1194 | 1 | P-M-M |
| 1195 | 1 | P-M-M |
| 1226 | 1 | P-M-M |
| 1231 | 1 | P-M-M |
| 1233 | 1 | P-M-M |
| 1298 | 1 | P-M-M |
| 1326 | 1 | P-M-M |
| 1358 | 1 | P-M-M |
| 1387 | 1 | P-M-M |
| 1871 | 1 | P-M-M |
| 1937 | 1 | P-M-M |
| 1949 | 1 | P-M-M |
| 1982 | 1 | P-M-M |
| 1990 | 1 | P-M-M |

Table 31

After Increasig Depth

From the table above its clear that all of these elements have failed during earthquake. Failure of these elements can initiate progressive collapse as these elements are columns(supporting vertical as well as lateral load). Above results indicate that the columns diamensions also needs to be upgaded as some members have failed, which is unaaceptable.  The stiffness (M2,M3) of the columns is increased by 50% and the analysis is re run.

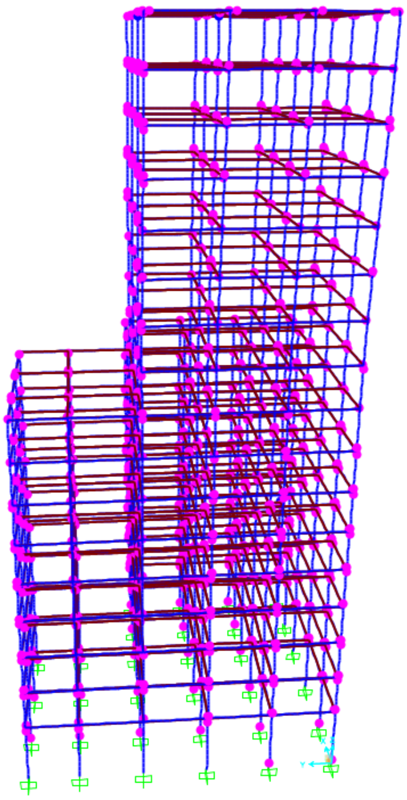

Fig 22

After increasing the stiffness of column by 50%, no column failed. All the columns are in Immediate Occupancy state. Which indicates that the frame is yielded but still has the capacity to resist lateral load as well as gravity load with negligible residual drift.

# CHAPTER 6

# CONCLUSION

From results of Modal combination Pushover Analysis and NLTHA following observations are made:

1. The Design results of a tall building structure should be verified even if the deciding parameters are within the prescribed limits. This can be done by a pushover analysis and NLTHA.
2. The results of Modal Combination pushover analysis are more reliable than the conventional methods of conducting Pushover analysis. It can be used to estimate performance of a structure.
3. Ductility is as much important as strength of the lateral load resisting elements.
4. Non Linear Time History Analysis gives most accurate results.
5. Special attention must be given if the structure have significant higher modes participations.
6. Concrete strength degrades under repetitive reverse cyclic loading. Hence just designing the structure for a peak ground acceleration isn't the best idea. Rather the structure should be designed for a number of reveasals for a given peak ground acceleration. So that the reverse sclic strength degradation can be taken into account. Indian Standard 1893 should make it clear if 0.36 PGA is single jerk or averaged of the complete time history analysis.
7. For near field sources, top most part of the building is damaged more serverly.
8. For far away sources, mid and lower part of the structure is damages. Drift is also higher in the same portion.

## References


1. FEMA 356 (2000), Pestandard and commentary for the seismic rehabilitation of buildings

2. Priestley, M.J.N. and Kowalsky, M.J., (2000). Direct Displacement-Based Seismic Design of Conrete Building. Bulletin of The New Zealand Society For Earthquake Engineering.

3. Priestley, M.J.N., Calvi, G.M., and Kowaisky, M.J., (2007). Displacement-Based Seismic Design of Structures.

4. ATC-40, (1996). Seismic Evaluation and Retrofit of Concrete Buildings: Vol. 1. Applied Technology Council

5. SEAOC, (1995). A Framework for Performance-Based Design. Structural Engineers Association of California, Vision 2000 Committee

6. Krawinkler, H., (1999). Challenges And Progress in Performance-Based Earthquake Engineering

7. Zareian, F. and Krawinkler, H., (2012). Conceptual Performance-Based Seismic Design Using Building-Level and Story-Level Decision Support System. Earthquake Engineering & Structural Dynamics

8. Priestley, N., (2007). The Need for Displacement-Based Design and Analysis

9. Priestley, M.J.N. and Kowalsky, M.J., (1998). Aspects of Drift and Ductility Capacity of Rectangular Contilivar Structural Wall

10. Erol KALKAN and Sashi K. KUNNATH (2004), Method of modal combinations for pushover analysis of buildings

11. FAJFAR, P., (1999). Capacity Spectrum Method Based on Inelastic Demand Spectrum. Earthquake Engineering and Structural Dynamics

12. Moehle, J.P., (1992). Displacement-Based Design of Building Structures Subjected to Earthquakes. Earthquake Spectra

13. Chopra, A.K. and Goel, R.K., (2001). Direct Displacement-Based Design: Use of Inelastic Design Spectra Versus Elastic Design Spectra. Earthquake Spectra

14. Sullivan, T.J., Priestley, M.J.N., and Calvi, G.M., (2006). Direct Displacement-Based Design of Frame-Wall Structures. Journal of Earthquake Engineering

15. Chopra, A.K., (2012). Dynamics of Structres, Theory and Applications to Earthquake Engineering. 4th edition. USA, Pearson Education, Inc., publishing as Prentice Hall: ISBN 13: 978-0-13-285803-8. 944 pages

16. T.Paulay and Priestley, M.J., (1992). Seismic Design of Reinforced Concrete and Masonry Building. United States of America John Wiley & Sons, INC

17. SAP2000, (2014). CSI Analysis Reference Manual For SAP2000®, ETABS®, SAFE® and CSiBridge. CSI Computers & Structures, Inc. Berkeley, California, USA. ISO# GEN062708M1 Rev.11

18. Mander, J.B., Priestley, M.J.N., and Park, R., (1988). Theoretical Stress-Strain Model for Confined Concrete. Journal of Structural Engineering. 114(8): p. 1804-1826.